CALIFORNIA ENERGY COMMISSION

Energy Research and Development Division

FINAL PROJECT REPORT

Modeling Flexible-Mode Geothermal Energy Production in California

Comprehensive Physical-Chemical Modeling to Reduce Risks and Costs of Flexible Geothermal Energy Production

June 2023 | CEC-500-2023-042

PREPARED BY:

Primary Authors:
Jonny Rutqvist, Quanlin Zhou, Lehua Pan,
Nicholas Spycher, Patrick Dobson, Mengsu Hu

Energy Geosciences Division
Lawrence Berkeley National Laboratory
1 Cyclotron Road, Berkeley, CA 94720
510-486-5432
https://eesa.lbl.gov/

Contract Number: EPC-16-022

PREPARED FOR:
California Energy Commission

Chuck Gentry
Project Manager

Kevin Uy
Branch Manager
ENERGY GENERATION RESEARCH BRANCH

Jonah Steinbuck, Ph.D.
Director
ENERGY RESEARCH AND DEVELOPMENT DIVISION

Drew Bohan
Executive Director

ACKNOWLEDGEMENTS

The authors thank the California Energy Commission for funding, under agreement EPC-16-022, this research as part of Work for Others funding from Berkeley Lab, provided by the Director, Office of Science, of the U.S. Department of Energy under Contract No. DE-AC02-05CH11231. We thank Gene Suemnicht for sharing with us his knowledge of the Long Valley area and the Casa Diablo geothermal field. We thank Calpine Corporation, including Julio Garcia, for providing well and field data for The Geysers geothermal field, including data related to the curtailment test. Finally, we thank the Technical Advisory Committee for providing project guidance.

PREFACE

The California Energy Commission's (CEC) Energy Research and Development Division supports energy research and development programs to spur innovation in energy efficiency, renewable energy and advanced clean generation, energy-related environmental protection, energy transmission and distribution and transportation.

In 2012, the Electric Program Investment Charge (EPIC) was established by the California Public Utilities Commission to fund public investments in research to create and advance new energy solutions, foster regional innovation and bring ideas from the lab to the marketplace. The CEC and the state's three largest investor-owned utilities—Pacific Gas and Electric Company, San Diego Gas & Electric Company and Southern California Edison Company—were selected to administer the EPIC funds and advance novel technologies, tools, and strategies that provide benefits to their electric ratepayers.

The CEC is committed to ensuring public participation in its research and development programs that promote greater reliability, lower costs, and increase safety for the California electric ratepayer and include:

- Providing societal benefits.
- Reducing greenhouse gas emission in the electricity sector at the lowest possible cost.
- Supporting California's loading order to meet energy needs first with energy efficiency and demand response, next with renewable energy (distributed generation and utility scale), and finally with clean, conventional electricity supply.
- Supporting low-emission vehicles and transportation.
- Providing economic development.
- Using ratepayer funds efficiently.

Modeling Flexible-Mode Geothermal Energy Production in California is the final report for the Comprehensive Physical-Chemical Modeling to Reduce Risks and Costs of Flexible Geothermal Energy Production project (Agreement Number EPC-16-022) conducted by Lawrence Berkeley National Laboratory. The information from this project contributes to the Energy Research and Development Division's EPIC Program.

For more information about the Energy Research and Development Division, please visit the CEC's research website (www.energy.ca.gov/research/) or contact the CEC at ERDD@energy.ca.gov.

ABSTRACT

In this project, numerical modeling tools were developed and applied to study flexible-mode geothermal energy production from typical California geothermal systems. The project focused on the impact of conversion from steady baseload to flexible-mode production on technical challenges such as well integrity, reservoir performance, and mineral scaling and corrosion in production wells.

Mechanical well integrity modeling showed changes in temperature and pressure of trapped fluids that can potentially cause mechanical failure in casing, cement, and adjacent host rock. It was found that the biggest risk of mechanical failure occurs during the initial startup of production because of large and rapid temperature increases from initially cool temperatures near the ground surface. However, if production cycling is carefully controlled, e.g., ramping up production slowly and not completely shutting down production, these impacts on the well assembly can be minimized.

The reservoir modeling showed little impact of variable production on reservoir performance because of limited pressure and temperature perturbations in the reservoir. Reservoir performance is affected by cold-water injection into geothermal reservoirs since the fracture-matrix heat exchange is a function of the shape and size of low-permeability matrix blocks and flow channels (e.g., fractures, fracture zones). The reservoir away from injection wells often acts like a single continuum with equilibrated temperature, which retards thermal breakthrough.

The reactive chemistry modeling showed that mineral scaling and corrosion can be controlled by keeping the wellhead pressure above the saturation pressure, while at the same time keeping the temperature above the silica saturation temperature. In a steam-dominated system, corrosion can be limited by avoiding condensation that can occur during production curtailment.

The modeling tools developed and demonstrated in this project can be applied to any new geothermal sites to develop site-specific operational strategies for safe variable geothermal production at reduced costs.

Keywords: Geothermal, variable production, curtailment, modeling, well integrity, reservoir, scaling, corrosion, cement, casing, temperature, pressure, flow rate, liquid, vapor

Please use the following citation for this report:

Rutqvist, Jonny, Zhou, Quanlin, Pan, Lehua, Spycher, Nicholas, Dobson, Patrick, Hu, Mengsu. 2021. *Modeling Flexible-Mode Geothermal Energy Production in California*. California Energy Commission. Publication Number: CEC-500-2023-042.

TABLE OF CONTENTS

LIST OF FIGURES

Page

EXECUTIVE SUMMARY

Background

The State of California has adopted aggressive renewable energy policies, enacted through legislation such as Senate Bill 100 (SB 100, De León, Chapter 312, Statutes of 2018), the state's landmark mandate requiring that renewable and zero-carbon energy resources make up 100 percent of electricity retail sales by 2045. However, increased use of intermittent renewable energy sources, primarily wind and solar, also increases the inherent variability and uncertainty in electricity demand and resource availability; this drives the need for operational flexibility from other renewable energy sources, including geothermal.

Geothermal energy is one of the state's renewable energy sources. Geothermal power plants use steam or brine from underground hot-water reservoirs to generate electricity. The Geysers Geothermal Field, the world's largest geothermal field, is in Sonoma, Lake, and Mendocino counties and contains a complex of 15 geothermal power plants that draw steam from more than 350 wells. Other major geothermal locations in California include the Salton Sea area in Imperial County, the Coso Hot Springs area in Inyo County, and the Mammoth Lakes area in Mono County.

Geothermal energy has traditionally supplied baseload power. However, with well-structured and appropriately priced contracts, geothermal plants can provide both baseload and flexible-mode electricity. The advancement of power plant and control technology allows geothermal power plants to operate in several variable modes including grid support, regulation, load following, spinning reserve, non-spinning reserve, and replacement or supplemental reserve (Matek, 2015). These modes are commonly referred to as ancillary services (Edmunds et al., 2014; Edmunds and Sotorrio, 2015). Flexible-mode operation of geothermal power plants will be particularly important for California's future electricity grid, which will be dominated by intermittent energy resources.

Flexible-mode geothermal energy production involves rapid energy production fluctuations by quickly reducing generation and restoring full production again after only a short time. Converting production from steady baseload to variable flexible-mode may also, however, negatively impact the system in some ways including corrosion and mineral deposition (scaling) in wells or mechanical damage fatigue to either well components or the reservoir.

A deeper understanding of the possible impacts of flexible-mode production on the reservoir-wellbore system is needed to ensure safe and sustainable geothermal energy production. This is important when considering that geothermal plants may have operated for decades on systems designed for baseload production, so operators may be overly cautious when switching from baseload to flexible-mode.

Project Purpose

The goal of this project was to develop modeling tools to comprehensively investigate the impacts of flexible-mode geothermal energy production on the many existing technical challenges of baseload operations including wellbore and reservoir integrity, scaling and corrosion of wellbores and pipelines, and flow and transport under the influence of injection and production.

The project covered broad research activities for both steam- and liquid-dominated geothermal systems for this general-purpose assessment. The project team conducted site-specific research for The Geysers geothermal field, which is steam-dominated, and used field data from pilot-scale tests of flexible-mode energy production, conducted by Calpine Corporation (majority owner of The Geysers) as part of a separate California Energy Commission-funded project (Urbank and Jorgensen, 2016). These modeling tools can help operators and technical consultants develop new site-specific operational strategies for safe, economic variable geothermal energy production. The tools and results achieved will provide greater electric grid reliability; increased integration of intermittent renewable energy; greenhouse gas emission reductions; and lower costs, all of which will benefit California ratepayers.

Project Approach

The project team created modeling tools and performed physical-chemical modeling to develop production strategies that reduce both the risks and costs of flexible geothermal energy generation. Steady production was first modeled for 100 days, which was sufficient to achieve conditions for a steady-state production rate including steady-state temperature and pressure conditions within the production well. A variable production rate was then simulated assuming a schedule of daily production cycles. Field data from The Geysers and Casa Diablo geothermal fields were used to ensure realistic field conditions in the model. Modeling challenges in investigating the impacts of flexible-mode geothermal energy production included (1) coupling the fluid and heat flow in the reservoir and the wellbores with geomechanics in the wellbore components and the reservoir, and (2) accurately modeling heat exchanges between fractures and matrix blocks in the reservoir. The improved modeling tools allowed efficient and accurate modeling of key coupled processes in both the reservoir and the wellbore system.

In this project, Lawrence Berkeley National Laboratory applied the modeling tools to quantify reservoir-wellbore geomechanical and geochemical processes during flexible-mode production pilot tests at the steam-dominated geothermal system at The Geysers geothermal field. This modeling approach was also applied to flexible-mode production from liquid-dominated geothermal systems based on field conditions at the Casa Diablo geothermal power plant near Mammoth Mountain, California, on the east side of the Sierra.

A technical advisory committee was assembled with scientists specializing in multiphase flow processes and risk analyses including wells and reactive geochemical processes, and included a representative from the owner of The Geysers Geothermal Field (Calpine Corporation), and a representative from the Casa Diablo Power Plant (Ormat Technologies, Inc.).

Project Results

In this project, numerical modeling tools were developed and applied to study the impacts of flexible-mode geothermal energy production on existing technical challenges such as well integrity, reservoir performance, and scaling and corrosion in production wells. Program routines as well as manuals were also developed so that these modeling tools can be applied to an analysis of both baseload and flexible-mode geothermal energy production.

Modeling simulations of both steady and variable geothermal energy production was performed for typical California steam- and liquid-dominated geothermal systems. These

simulations validated application of the modeling tools and provided important conclusions for managing variable geothermal energy production. These results provide guidance to optimize production without negatively impacting either production or system components, including wells.

The modeling showed that temperature fluctuations are the driver that could lead to negative impacts on both mechanical well integrity and mineral scaling and casing corrosion. Modeling further revealed that the highest thermal perturbation occurred in production wells at shallow depth, just below the ground surface. Temperature changes in the cement behind casings can cause significant fluid pressure changes due to thermal expansion of trapped fluids, which could in turn severely impact the mechanical integrity of the well assembly.

The biggest risk of mechanical well integrity occurred during the initial start-up of production because of a large and rapid temperature increase from a relatively low temperature near the ground surface. During variable production with daily production cycles, temperature fluctuations also caused fluctuations in pore pressure and stress. These stress fluctuations were larger when producing from a very hot steam-dominated system. However, modeling results also showed that if production cycling is carefully controlled, impacts on the well assembly can be minimized. Mechanical well integrity issues can be minimized by avoiding abrupt changes in production (e.g., by ramping up hot fluid production slowly and avoiding full production shutdowns).

Flexible production had little impact on geothermal reservoirs because there was no impact on reservoir temperature near the relevant production well and the pressure perturbations induced by daily production rate variations were limited only within near-well regions (when compared with constant-rate production). Flow and heat transport modeling showed that cold-water injections significantly impacted reservoir temperatures. The thermal travel distance of cold water depends on fracture-matrix heat exchange that is a function of the shape and size of matrix blocks of low permeability and of flow channels (fractures and fracture zones). Early thermal breakthrough is possible for channelized flow through fracture zones that are meters wide. Otherwise, fractures and matrix blocks act like a single continuum for heat transport because they are in temperature equilibrium in a short time, away from injection wells.

Mineral scaling and corrosion can be controlled by maintaining wellhead pressure above saturation pressure and at the same time keeping the temperature above the silica saturation temperature. In a steam-dominated system, corrosion can be minimized by avoiding condensation that could form during prolonged production curtailments.

The modeling tools developed and demonstrated in this project can be applied to either existing or new geothermal sites to develop site-specific operational strategies and to design production cycling for safe, variable geothermal production.

Technology/Knowledge Transfer/Market Adoption (Advancing the Research to Market)

The project team at Lawrence Berkeley National Laboratory developed materials to spur technology transfer, such as project fact sheets, reports, conference and journal articles, and presentation materials. Modeling tools developed in this project have been documented in reports and scientific articles and presented at conferences. Potential users of these modeling

tools are scientists and engineers familiar with analytical and numerical modeling of subsurface thermal, hydraulic, and geomechanical processes. To communicate the methods, technologies, and learnings developed in this project, a number of technology/knowledge transfer activities were planned and carried out. These included presentations at the Stanford Geothermal Workshop (2018 and 2020) and the World Geothermal Congress (2021), which were attended by representatives from industry, academia, and government agencies. The presentations were well attended and of interest to many operators as revealed by the discussions following the presentations. Moreover, discussions and meetings have been carried out with project partners at Calpine Corporation and Ormat Technologies, Inc. Finally, representatives from both Calpine and Ormat were members of the project's technical advisory committee.

Benefits to California

This project provides geothermal energy producers with tools and guidelines that can ultimately lead to greater grid reliability, increased use of intermittent renewable energy, reductions in greenhouse gas emissions, lower costs, and other benefits. More in-depth knowledge on how to optimally and safely run a geothermal plant in flexible-mode provides reliability and will allow for better use of the current installed capacity, as currently just 48 percent of the capacity is in operation year-round (Note that capacity factors for these plants vary significantly from field to field [Robertson-Tait et al., 2021]). Flexible-mode operations can also be cost effective when compared with alternative solutions involving energy storage. The importance and the cost effectiveness of flexible-mode geothermal production will become greater as intermittent renewable energy gains dominance in the state's energy supply. This project will provide a return on investment for California electric ratepayers and other stakeholders such as the California Public Utilities Commission and investor-owned utilities. If the tools and findings gained from this project are adopted to enable safe and efficient flexible-mode geothermal operations, the investment could be returned from energy sales revenue in just a few months.

CHAPTER 1: Introduction

Project Background

Operational Flexibility Need and Demonstration

Geothermal power plants have traditionally generated baseload power. With well-structured and appropriately priced contracts, however, geothermal power plants can provide both flexible and baseload power; the advancement of power plant and control technologies allows geothermal power plants to operate in several variable modes including grid support, regulation, load following, spinning reserve, non-spinning reserve, and replacement (or supplemental) reserve (Matek, 2015). These modes are commonly referred to as ancillary services (Edmunds et al., 2014; Edmunds and Sotorrio, 2015). The flexible-mode operation of geothermal power plants will be important for reliable operation of the state's electricity grid, which will be increasingly dominated by intermittent energy resources.

Flexible geothermal operations have been demonstrated at the Puna Geothermal Venture plant in Hawaii since 2012 (Nordquist et al., 2013). This plant, the first of its kind, provides ancillary grid support services identical to existing oil-fired peak generating resources on Hawaii's Big Island. A research and development project was funded by the California Energy Commission (CEC) in 2015 to investigate variable-energy generation capabilities at Northern California's The Geysers geothermal power plants, with pilot tests of variable energy production and field management strategies for flexible-mode generation.

Challenges of Baseload and Flexible-Mode Geothermal Production

For traditional baseload operation of geothermal power plants, challenges include: production well scaling caused by mineral deposition at steam-water interfaces, corrosion of wellbores and steam pipelines, and wellbore integrity and geomechanical damage caused by pressure and temperature perturbations (ΔT). Moreover, cold-water injection can affect the reservoir near the injection well and between the injection and production wells, including dissolution and transport of non-condensable gases (NCGs). All these impacts depend on the characteristics of the geothermal reservoir systems, such as either steam- or liquid-dominated reservoirs, high or low concentrations of NCGs and total dissolved solids (TDS), in situ pressure and temperature reservoir conditions, and reservoir rock properties. This means that some of these impacts are site specific. For example, scaling is a serious issue in the Salton Sea geothermal system in California, with its hypersaline brines, while it is not a big issue at The Geysers geothermal field, which is a steam-dominated reservoir.

When the baseload operation of an existing geothermal plant switches to flexible-mode production, or when a new plant starts with flexible-mode operation, those challenges may differ from those for baseload operation. One of the main challenges and concerns related to conversion from baseload to flexible-mode operation is wellbore integrity. Flexible-mode geothermal production typically includes daily production cycles that heavily stress the wellbore and reservoir system. The detrimental effect of thermal stresses on casing is well established from years of experience in steam injection in heavy oil fields, though a

geothermal well poses even more complex loading issues (Teodurio, 2015). In all scenarios, the heating and cooling process creates the expansion and shrinkage of all materials in the well. The casing is especially affected by temperature changes since metals provide higher thermal expansion coefficients than cement. Cyclic thermal loading during rapid changes in flexible-mode production may lead to fatigue in both the casing and cement (Teodurio, 2015; Kaldal et al., 2015). There is therefore a need to investigate the effects of flexible-mode production on well integrity over the operational life of a geothermal field to determine how to optimize the total production and production flexibility, at reduced risk and cost of well failure.

Another issue with flexible-mode production is how it affects scaling in production wells, corrosion of production wellbores, and steam condensation in pipelines when compared with baseload production. The precipitation of solid phases in geothermal wells and surface equipment (mineral scaling) is a well-known process that can significantly impair both the productivity and longevity of geothermal operations. Scaling typically results from boiling due to pressure decreases in production wells, which in turn releases CO_2 and H_2S, which cause pH increases that lead to deposition of carbonate and sulfide scales (Arnorsson, 1989; Spycher and Reed, 1989; Criaud and Fouillac, 1989; Reyes et al., 2002). High-temperature geothermal fluids (greater than about 392°F [200°C]) typically also contain elevated concentrations of dissolved silica, which can lead to the precipitation of amorphous silica and iron silicates upon cooling and evaporative concentration. In production wells, mineral precipitation typically occurs over a limited interval corresponding with the depth at which geothermal fluid boils (flashes) in the well. The potential for mineral scaling in wells depends upon production pressure and temperature variations as well as fluid chemistry. If pressures and temperatures are not maintained high enough during flexible-mode production, it will exacerbate mineral scaling. Corrosion can also plague geothermal operations, including deterioration of slotted liners and well casings by hot saline or acidic fluids, sulfur stress corrosion cracking, oxidation of H_2S at the well head leading to corrosion by sulfuric acid, corrosion by acid gases (e.g., HCl) partitioning in steam condensates in pipelines such as at The Geysers (Pruess et al., 2007) and carbonic acid in cooling towers (Kaya and Hosban, 2005). Although the effects of corrosion can be alleviated by selecting suitable materials for the construction of wells and other engineered systems, defining optimal operating conditions (e.g., pressure, temperature, composition space) can also help prevent serious corrosion problems.

Finally, injection and production schedule changes may also impact the reservoir. Flexible-mode production may change the thermal transients at the production wells, near the wellbore in the shallow formations, and in the reservoir. High-frequency and rapid transients need high-resolution modeling of near-wellbore perturbations. Injection of cold water induces significant ΔT along the injection well and within the fractured reservoir because of the considerable difference between in situ reservoir temperatures and injected water temperatures. The large ΔT will propagate, with time, from injection wells to production wells under the combined effects of advection with flowing fluid (water, steam, or both) and thermal conduction. In a fractured geothermal reservoir, working fluid mainly flows through connected fractures with advective heat transport, while thermal conduction mainly occurs in rock matrix blocks; heat gain from the rock matrix mainly depends on the fracture-matrix heat exchange. The heat gain for the flowing fluid slows down thermal drawdown at the production well, ultimately extending the lifespan of a hydrothermal field.

Project Objectives

The goal of this project was to comprehensively investigate the impacts of flexible-mode geothermal energy production on the many technical challenges that face baseload production including wellbore and reservoir integrity, scaling and corrosion of wellbores and pipelines, and flow and transport under the influences of injection and production.

Specific project objectives were to:

- Develop coupled reservoir-wellbore thermal-hydrological-mechanical-chemical (THMC) modeling tools to address specific problems.
- Evaluate wellbore and reservoir integrity using the coupled reservoir-wellbore thermal-hydrological-mechanical (THM) modeling.
- Develop improved methods to identify and address corrosion or scaling issues in wells and pipelines via reactive transport and geochemical modeling.
- Develop power plant and control technologies that allow geothermal power plants to operate in both baseload and flexible modes.
- Quantify production and injection impacts on geothermal reservoirs for both baseload and flexible-mode energy production.

The project covered broad research activities for both steam- and liquid-dominated geothermal systems for this general-purpose assessment. The project team conducted site-specific research for The Geysers geothermal field, which is steam-dominated, and used field data from pilot-scale tests of flexible-mode energy production, conducted by Calpine Corporation (majority owner of The Geysers) as part of a separate California Energy Commission-funded project (Urbank and Jorgensen, 2016). These modeling tools can help operators and technical consultants develop new site-specific operational strategies for safe, economic variable geothermal energy production. The tools and results achieved will provide greater electric grid reliability; increased integration of intermittent renewable energy; greenhouse gas (GHG) emission reductions; and lower costs, all of which will benefit California ratepayers.

CHAPTER 2:
Project Approach

The project team created modeling tools and performed physical-chemical modeling to develop production strategies that reduce both the risks and costs of flexible geothermal energy generation. This was accomplished by improving the Transport of Unsaturated Groundwater and Heat (TOUGH) family of codes for simulations required in this project (Pruess et al., 1999). The relevant module is the numerical simulator T2WELL (Pan and Oldenburg, 2014) for coupled reservoir-wellbore multiphase multicomponent flow and transport modeling. This was coupled with the geomechanical simulator Fast Lagrangian Analysis of Continua in 3 Dimensions (FLAC3D) (Itasca, 2011). The improvement of modeling capabilities included coupling FLAC3D with T2WELL for THM modeling in both reservoirs and wellbores, and coupling analytical modeling of multi-rate conduction processes in matrix blocks with analytical solutions of convection-dispersion in fractured reservoirs.

The modeling of mechanical well integrity was approached by coupling the T2WELL reservoir-wellbore simulator with FLAC3D geomechanical simulator. Lawrence Berkeley National Laboratory's (LBNL) T2WELL is a numerical simulator that can accurately simulate fluid and heat flow in both wellbores and reservoirs (Pan and Oldenburg, 2014), including complex 2-phase flow phenomena such as condensation or evaporation, counter flow, and gas lifting. FLAC3D is an advanced geomechanical simulator (Itasca, 2011) that has previously been linked to several of LBNL's TOUGH suite of codes for modeling coupled multiphase fluid flows and geomechanical processes (Rutqvist, 2011; 2017), including extensive applications to the high-temperature geothermal system at The Geysers (Rutqvist et al., 2016). Using T2WELL linked with FLAC3D enables accurate modeling of multiphase flow processes within the wellbore and the effects of wellbore pressure and temperature changes on the well (including casing and cement), as well as in the surrounding rock.

Second, LBNL also developed geochemical and reactive transport numerical models such as CHILLER (Spycher and Reed, 1992) and TOUGHREACT (Xu et al., 2011; Sonnenthal et al., 2014) which are specifically designed to investigate the coupled effects of pressure, temperature, fluid and rock composition, and flow variations on mineral precipitation and dissolution, along with other chemical reactions related to corrosion. These models could be used to investigate the effects of flexible production scenarios on scaling and corrosion in California's geothermal fields.

Finally, for modeling the impact of injection and production on the reservoir, new analytical solutions were developed to better simulate the non-isothermal flow and transport along injection and production wells and in fractured geothermal reservoirs. This was motivated by the fact that the first-order approximation used in current dual-porosity or dual-permeability models may result in large simulation errors for fracture-matrix heat exchange. The approximation error in the dual-porosity modeling will result in earlier and larger thermal drawdown in simulated production wells. For flexible-mode geothermal energy production, highly accurate models are needed to capture the large thermal transients with more temporal variations. This was accomplished by developing a new Fortran module (SHPALib) to include multi-rate mass transfer-like processes (e.g., thermal diffusion). The SHPALib module can be

used to analytically simulate the diffusion processes (e.g., hydraulic, thermal, and solute diffusion) within matrix blocks, as well as advection-dispersion-diffusion in the fracture continuum (Zhou et al., 2017a, b, 2019).

The developed modeling tools were applied to various scenarios of geothermal production and water injection in both liquid- and steam-dominated reservoir systems. A multi-scale modeling approach was employed to focus on geomechanical behavior and wellbore integrity in the high +ΔT zone, geomechanical behavior in the high -ΔT zone, and wellbore scaling and corrosion in production wells. For example, T2WELL was applied to model the entire wellbore and the reservoir in an axisymmetric configuration for accurate modeling of 2-phase flow phenomena such as condensation or evaporation, counter flow, gas lifting, and temperature evolution in the reservoir and well (including casing, cement and surrounding rock). Geomechanical analyses were conducted for the high +ΔT zone. Thus, full coupled THM analysis using T2WELL-FLAC3D focused on parts of the system for an accurate analysis of its most critical components. Moreover, the chemical analysis of casing corrosion and scaling was performed on the local scale in parts of the system with input of pressure, saturation, and temperature evolutions from large-scale simulations.

The short- and long-term impacts of injection and production on reservoir performance were modeled using the SHPALib forward simulator. Using this improved model, the fracture-matrix thermal transfer, and near-wellbore and in-reservoir thermal perturbations can be accurately simulated, which is of critical importance in geothermal energy production. With the new SHPALib module for fracture-matrix interaction, the research team was able to capture rapid changes near production wells associated with flexible-mode production (Zhou et al., 2017a, b, 2019). All of this modeling and assessments were conducted for idealized liquid- and steam-dominated geothermal reservoir systems, and for analyzing flexible-mode geothermal production and water injection using the field pilot test data from the steam-dominated Geysers geothermal field.

CHAPTER 3:
Project Results

Development and Testing of Modeling Tools

The goal to develop novel modeling tools tailored for analyzing reservoir-wellbore coupled processes was achieved and documented in the "Modeling Tools Report" submitted and documented in Rutqvist et al., (2018a). Specifically, the completed adaptations and improvements of the modeling capabilities included:

(1) Coupling the T2WELL reservoir-wellbore simulator with the FLAC3D mechanical simulator for modeling coupled THM processes and well integrity issues.

(2) Coupling analytical modeling of multi-rate conduction processes in matrix blocks with analytical solutions of convection-dispersion in fractured reservoirs.

The developed T2WELL-FLAC3D simulator is based on linking two existing simulators: T2WELL and FLAC3D (Figure 3-1). T2WELL is a numerical simulator that can accurately simulate fluid and multiphase flow processes within the wellbore and effects of wellbore pressure and temperature changes on well integrity (including casing and cement) as well as in surrounding rock. The combination of these two codes makes it possible to quantitatively evaluate the impact of baseload injection and production and flexible production on the mechanical integrity of the well assembly (Rutqvist et al., 2018b).

The developed fracture-matrix heat transfer models were critical for modeling near-field reservoir behavior during variable geothermal energy production. Figure 3-2 shows a conceptual model of fracture-matrix interaction that can be effectively modeled with the adopted approach. The analytical models were developed for simulating the diffusive heat flux from fractures to single matrix blocks, and simulating heat transport through fractured reservoirs with fracture-matrix heat exchange considered analytically (Zhou et al., 2017a, b; 2018; 2019).

The developed T2WELL-FLAC3D simulator was tested and demonstrated by modeling steady and variable geothermal production for generic cases related to both steam-dominated and liquid-dominated geothermal systems (Rutqvist et al., 2018c; 2020a). The developed modeling capabilities for the analysis of multi-rate heat transport in fractured reservoirs were tested by running a number of general test cases. Users' manuals were completed with instructions on how to use T2WELL-FLAC3D and SHPALib models. Finally, the CHILLER software (Spycher and Reed, 1992) was tested for geochemical simulations of mineral scaling under variable pressure and temperature conditions.

Figure 3-1: Coupled T2WELL-FLAC3D Analysis of Well Integrity

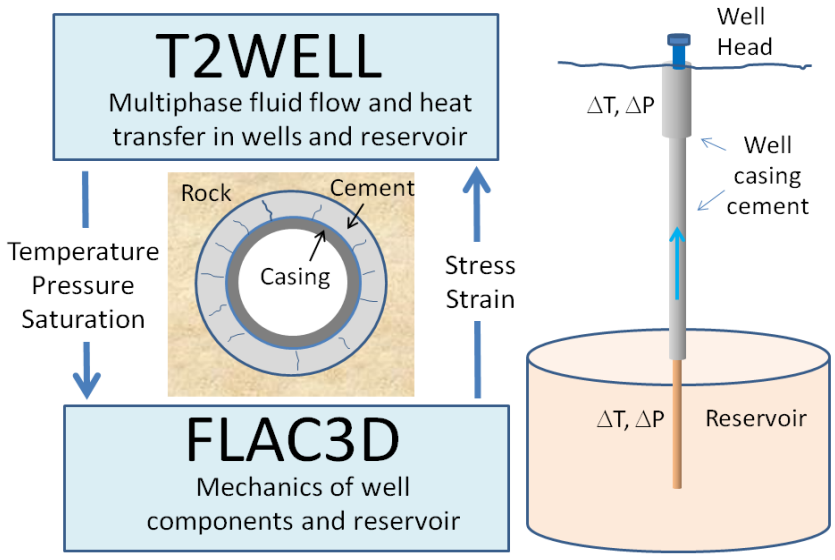

Coupling and interactions between T2WELL for reservoir-wellbore multiphase flow and multicomponent transport modeling and FLAC3D for geomechanical modeling, with application to wellbore integrity analysis by including reservoir, wellbore, and high +ΔT zone (Rutqvist et al., 2018b).

Source: LBNL

Figure 3-2: Modeling Heat Transport With Fracture-Matrix Interaction

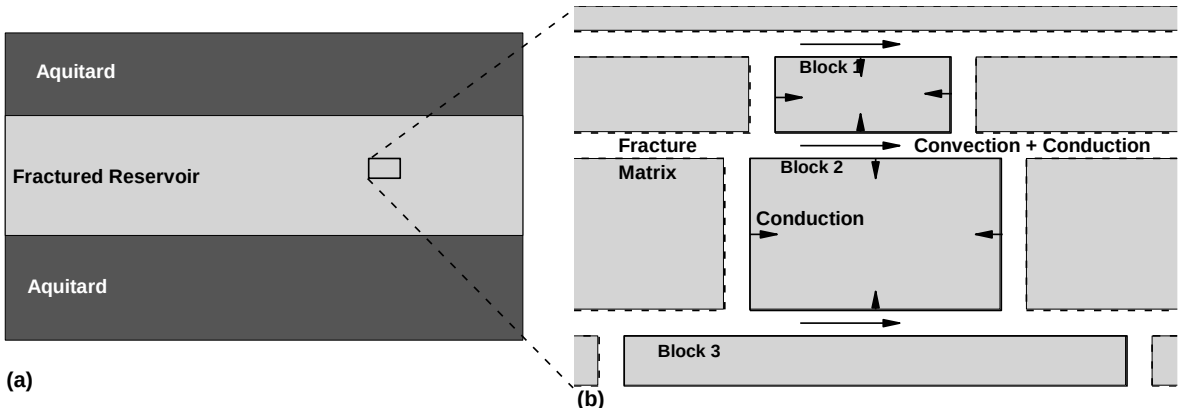

Conceptual model of fracture-matrix interaction problem that can be effectively solved using the developed SHPALib code. (a) A fractured reservoir bounded by aquitards or a fracture zone embedded in the rock matrix, and (b) a portion of the REV consisting of fractures and matrix blocks of different shapes and sizes, as well as heat convection-conduction in fractures coupled with heat conduction in matrix blocks (Zhou et al., 2017a, b, 2018, 2019).

Source: LBNL

Impact on Well Integrity

This section explains the impact of steady and flexible-mode geothermal production on mechanical well integrity and the potential for corrosion and mineral deposition (scaling) in wells. Both steam- and liquid-dominated geothermal systems were considered, using data from The Geysers and Casa Diablo geothermal fields. The T2WELL-FLAC3D and CHILLER modeling tools were applied.

Thermal-Hydraulic Analysis of Temperature and Pressure Responses

An initial set of simulations were performed with T2WELL to model the basic temperature and pressure responses associated with variable (cyclic) geothermal production. The research team considered both steam- and liquid-dominated geothermal systems, with well design, field data, and conditions from The Geysers and Casa Diablo geothermal fields. An important step for realistic modeling of pressure and temperature changes in the system was to calibrate the model against field data to set up accurate initial conditions and match steady production data. The simulations were then conducted by modeling steady production for 100 days to obtain pseudo steady-state conditions of temperature in the wellbore assembly and surrounding geological formations. Thereafter, variable production conditions were initiated in the model simulations and continued for 100 days. The well designs were obtained from the California Division of Oil, Gas, and Geothermal Resources (CA DOGGR [now CalGEM]) GeoSteam database.

Steam-Dominated System (Northwest Geysers)

For the steam-dominated system, well design, geology and production data from a well at The Geysers was used to ensure realistic field conditions in the model (Rutqvist et al., 2018c). These data were from well Prati 25 (P25), which is one of the production wells associated with the Northwest Geysers EGS Demonstration Project (Garcia et al., 2016). The Northwest EGS Demonstration site was well characterized. Extensive modeling was conducted of reservoir pressure, temperature, and reservoir responses to steam production and liquid fluid injection (Garcia et al., 2016; Rutqvist et al., 2016). The main steam reservoir, known as the "normal" temperature reservoir at The Geysers, typically has a temperature of about 464°F (240°C) and steam pressure of about a few megapascals (MPa). Figure 3-3 shows the P25 well design and geological layering that were both important inputs to the study's modeling.

An initial simulation was conducted using a steady production rate based on the P25 well data on production rate, wellhead pressure, and temperature to ensure realistic field conditions. The wellhead pressure and temperature were matched for a given water mass production by calibrating reservoir permeability.

Figure 3-4 shows the evolution of temperature and pressure in the cement behind the casing for the case of a constant-rate steam production of 8 kilograms per second (kg/s). The temperature increases rapidly to over 392°F (200°C) within a few days of initiation of production. The temperature change, ΔT, is the highest in the shallowest part of the well because of a relatively low initial temperature. At 2.4 meters (m) below the ground surface, $\Delta T \approx 200°C$, while at 527 m depth, $\Delta T \approx 130°C$ (Figure 3-4a). The rapid temperature increases also led to thermal pressurization due to thermal expansion of the fluid in a low permeability medium. Figure 3-4b shows that pressure increases by as much as 60 MPa at 2.4 m depth with the peak pressure occurring on the second day of production. This appeared to be a very

substantial pressure increase that would be very important to consider in a well integrity analysis. The amount of pressure increase depends on both the rate of temperature increase and the permeability of the cement. The fact that the cement in the upper part of the well is confined between two steel casings makes this high thermal pressurization possible. Thus, the well design and material properties, including permeability and pore-compressibility, are important for accurately predicting these effects.

Figure 3-3: Well Design and Geology for a Steam-Dominated System

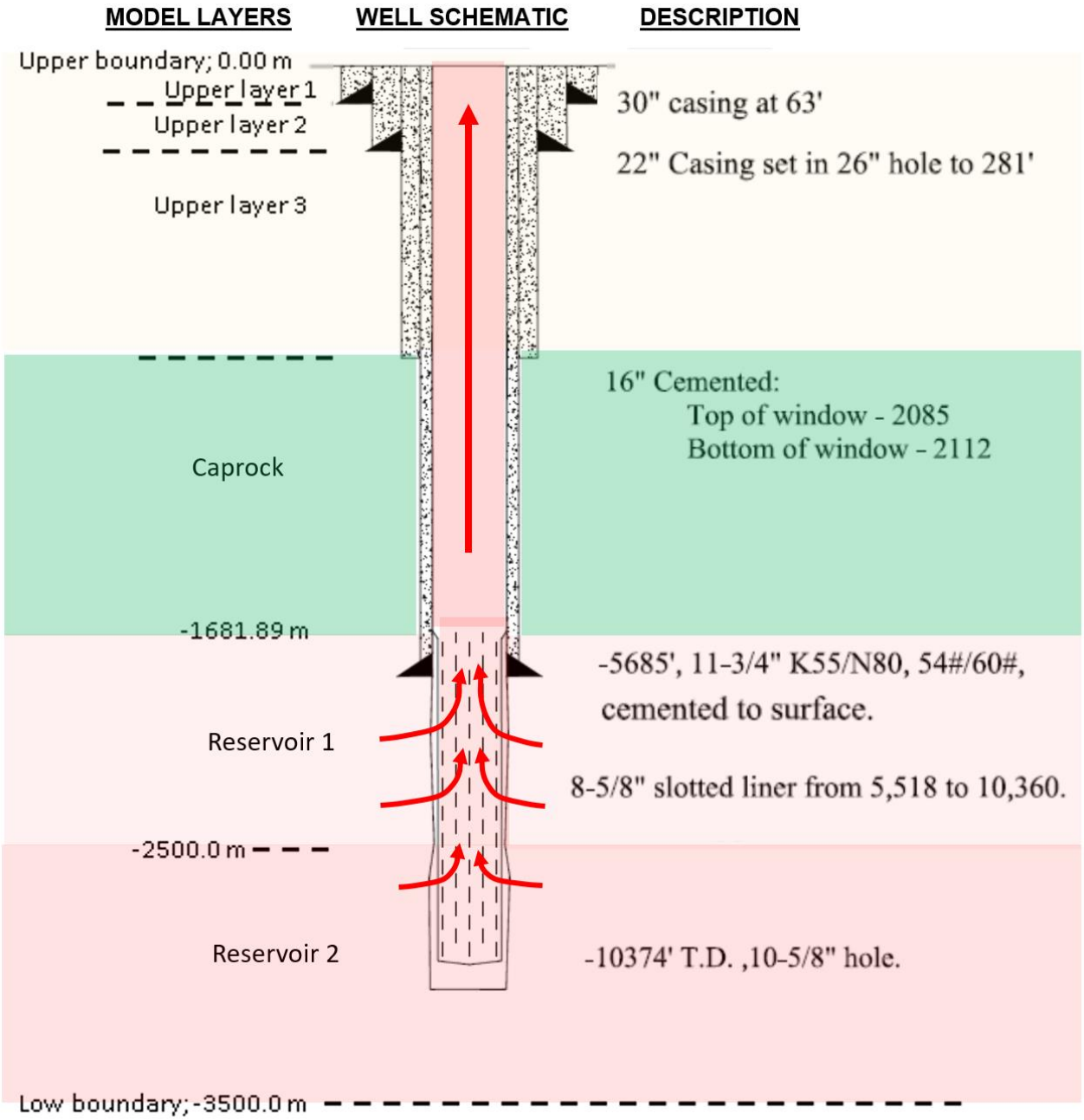

P25 well design at the Northwest Geysers and model layers used in T2WELL for simulation of constant- and variable-rate geothermal production.

Source: LBNL

Figure 3-4: Steady Production Response in Cement Behind Casing

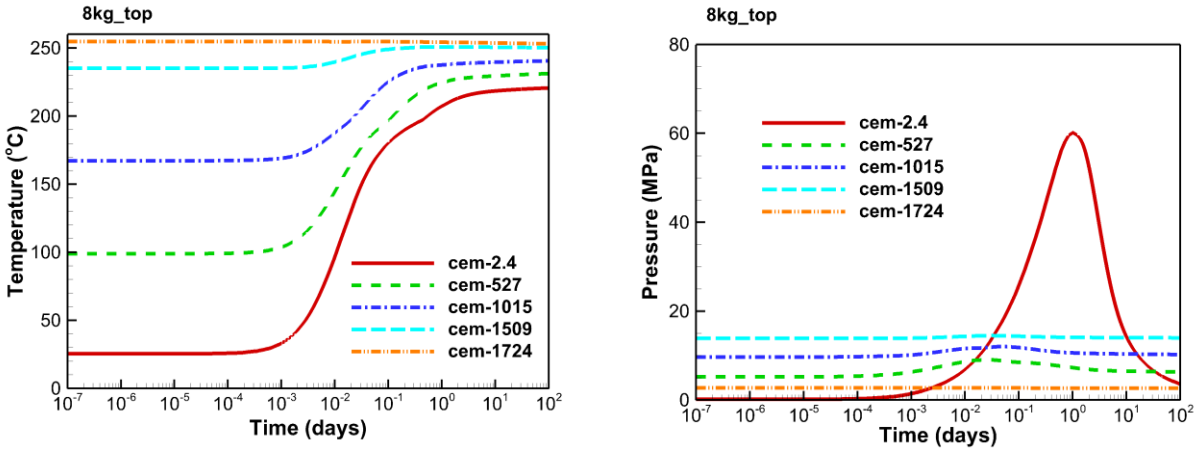

(a) (b)

Simulation results for the base case of 100 days of production at a rate of 8 kg/s from a deep geothermal well in a steam-dominated field. (a) Temperature and (b) pressure evolutions within the cement behind the innermost casing at different depths below the ground surface (see legend, in meters).

Source: LBNL

The variable production was simulated by a number of different schedules as a sensitivity analysis. Figure 3-5 presents an example of variable schedule of 14 hours peak rate (12.00 kg/s) followed by 10 hours off-peak rate (5.14 kg/s) during weekdays, and 24 hours off-peak rate (5.14 kg/s) during weekends. Using this production schedule, the average production would remain equivalent to the preceding constant production rate of 8 kg/s (Figure 3-5a). As a result of the variable production, the temperature fluctuates by about 4°C to 5°C at the wellhead and within the cement just behind the innermost casing (Figure 3-5b). These temperature fluctuations also result in pressure fluctuations of up to 2 MPa. Interestingly, the pressure oscillations in the cement behind the casing were much greater than the steam pressure oscillations within the borehole itself. The team also observed that the pressure oscillations in the cement decline with time; the magnitude of oscillations was about 2 MPa after 10 days, but as low as 1 MPa after 70 days. The T2WELL simulation shows that this decline is associated with the presence of a gas bubble within the cement, indicating the importance of water being driven out from the cement (Figure 3-6). It also indicates the importance of liquid saturation in the cement behind casing. The thermal pressurization with high-pressure changes would occur only if cement behind the casing is liquid saturated or nearly liquid saturated.

Figure 3-5: Variable Production Responses in the Well

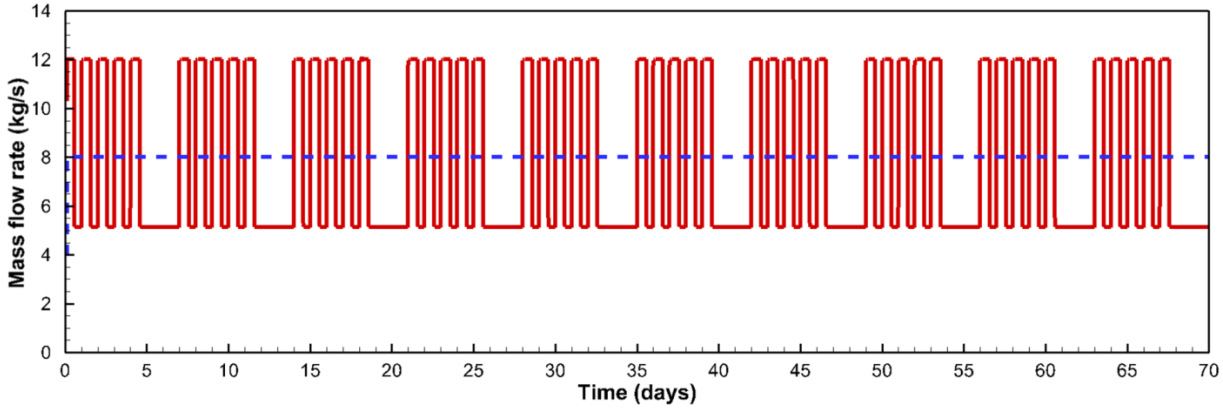

(a)

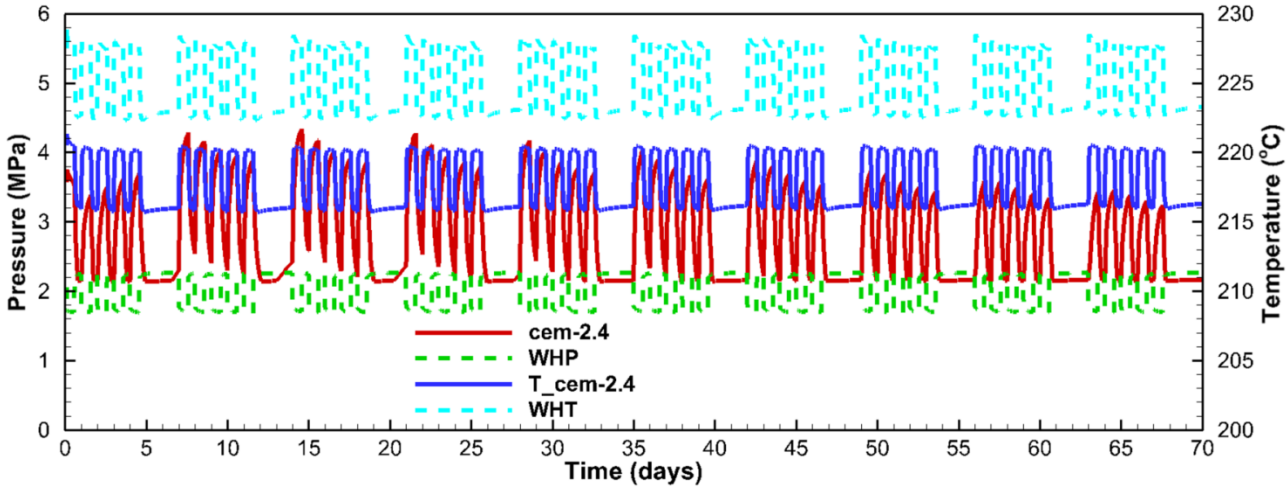

(b)

Evolution of (a) mass flow rate and (b) pressure (cem-2.4) and temperature (T_cem2.4) in cement behind the modeled casing at 2.4 m depth for an assumed variable production rate schedule, and wellhead pressure (WHP) and temperature (WHT).

Source: LBNL

Figure 3-6: Variable Production Response in Cement Behind Casing

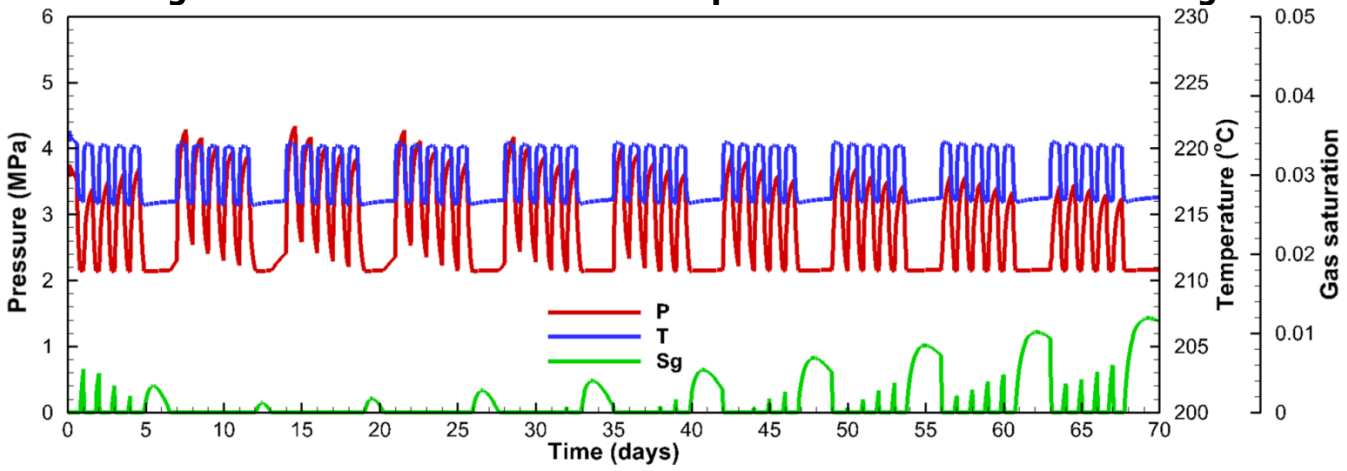

Evolution of pressure (P), temperature (T) and gas saturation (Sg) in cement behind the modeled well casing, showing the impact of a gas bubble and water driven out of the cement.

Source: LBNL

Liquid-Dominated System (Casa Diablo)

Field data from the Casa Diablo geothermal field in the Long Valley Caldera, California, were used to develop realistic conditions for the simulations of a liquid-dominated geothermal system (Rutqvist et al., 2020a; 2021). The geothermal power plants at Casa Diablo are binary due to moderate temperature reservoir fluids. In this study, researchers used well geometry and conditions from well MBP-4, which is a relatively shallow well with a total depth of 205 m. The design of production well MBP-4 was adopted, while data from a number of adjacent wells were used to derive reasonable initial reservoir conditions for the modeling. The design of the MBP-4 production well is shown in Figure 3-7, along with geologic stratigraphy. Production occurs from an open borehole section with a slotted liner extending from 126 to 205 meters depth, with a downhole pump (shaft turbine pump) to maintain well pressure.

The initial conditions of pressure and temperature were established based on early production field data at the Casa Diablo geothermal field (Miller and Vasquez, 1988), including the measured temperature profile in well MBP-3 (located about 60 m away from the MBP-4 production well) (Farrar et al., 2010). The geological unit denoted as "HotZone" is the main feed zone of the reservoir. The permeability of this zone was adjusted manually by matching the simulated initial reservoir pressure and flowing bottom hole pressures to data measured during a well production test (MBP-4) performed on July 6, 1984. All other parameters are from the literature or are best estimates for similar types of materials.

The research team first conducted thermal-hydraulic analysis of wellbore pressure and temperature responses, as well as production, for both baseload and flexible geothermal production. Steady production was first modeled for 100 days, which was sufficient to achieve conditions for a steady-state production rate and steady-state temperature and pressure conditions within the production well. A variable production rate was then simulated assuming a schedule of daily production cycles. The results from these thermal-hydraulic analyses (in terms of temperature, pressure and moisture content responses) were also input into the subsequent well integrity analysis and considered for evaluation of mineral scaling potential.

The base-case simulation of constant-rate production for 100 days at 1,500 gallons per minute (GPM) (84.31 kg/s) showed that the pressure loss from the well bottom to the well head was small due to downhole pumping, while temperatures increased substantially in the upper part of the well. This abrupt change in temperature caused heat loss into the well assembly and heating of the surrounding rock (Figure 3-8a). Pressure in the casing cement near the ground surface increased significantly as the cement was heated up by the hot water in the well and reached its peak at about one-half day, then decreased as the pressurized water was gradually driven out (Figure 3-8b). At the middle depth of the casing cement, the pressure increase was lower due to a lesser temperature difference, but the elevated pressure lasted much longer. All these changes in pressure within the well assembly were caused by thermal pressurization, which in turn depends on temperature evolution in the system. Thermal pressurization is the process of temperature-driven changes in pore pressure that occur because the thermal expansion of the pore fluid is much larger than the thermal expansion of the solid phase. This process tends to be more significant in a low-permeability porous media, like cement, because it takes a longer time for the pressurized fluid to diffuse.

Figure 3-7: Well Design and Geology for a Liquid-Dominated System

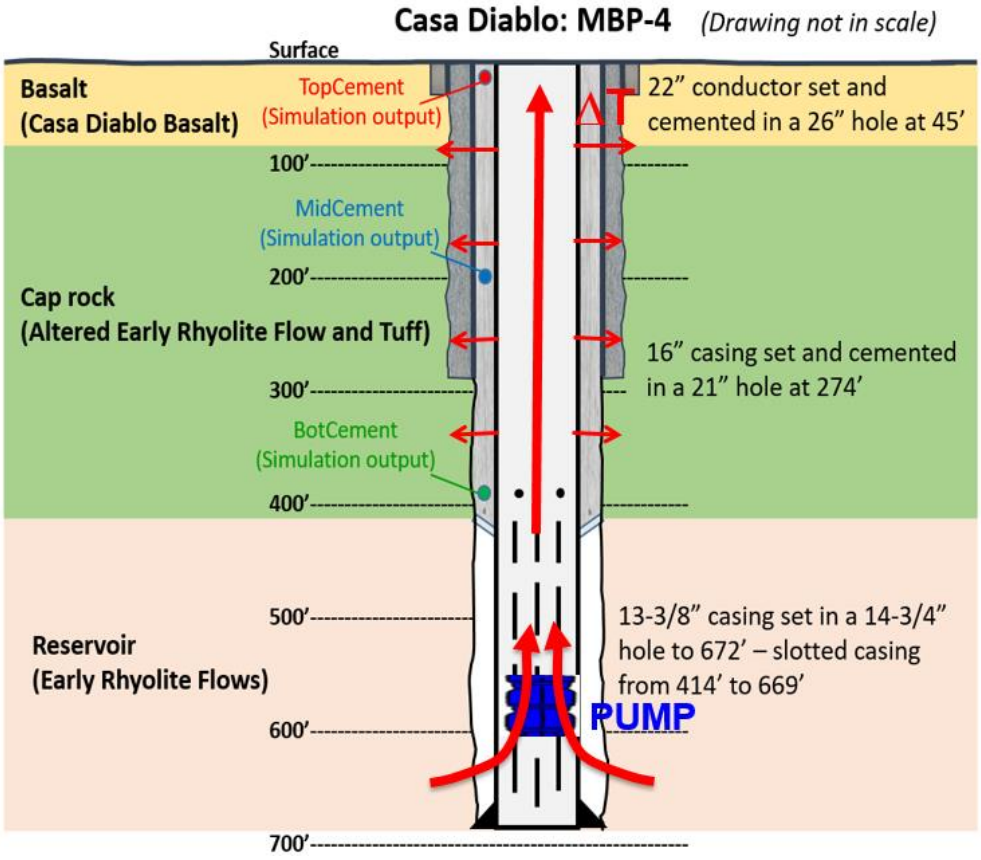

Casa Diablo MBP-4 production well geometry and geological units considered in the model (redrawn from DOGGR GeoSteam Data Base file).

Source: LBNL

Cyclic production was simulated for various scenarios of production cycles since the impact of cyclic production depends upon the magnitude and rate of production changes. Figures 3-9 through 3-11 show production rates, along with temperature and pressure responses within the well assembly. Here the team modeled cyclic production, with a peak rate of 1,600 GPM (89.93 kg/s) every 14 hours, followed by 10 hours off-peak at a rate of 700 GPM (39.34 kg/s) during weekdays, with 24 hours off-peak at 700 GPM (39.34 kg/s) during weekends. The weekly average production was 1,075 GPM (60.42 kg/s).

Figure 3-8: Steady Production Responses in Cement Behind Casing

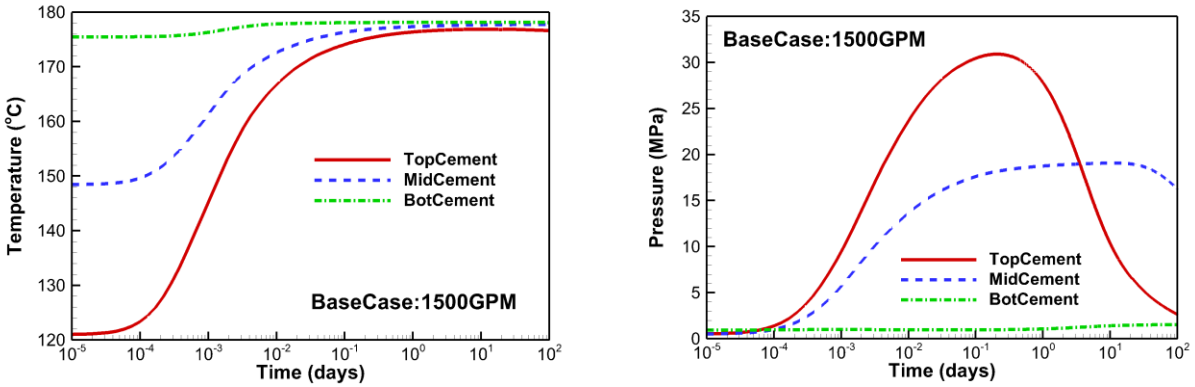

(a) (b)

Simulation results for the base case constant-rate production at 1500 GPM (84.31 kg/s) for 100 days; (a) temperature and (b) pressure in casing cement at three different depths. TopCement, MidCement and BotCement output locations within the cemented portions of the well completion are shown in Figure 3-7.

Source: LBNL

A slight undershot in wellhead production rate occurred when a high flow rate suddenly switched to a low rate from an induced shock wave in the well (Figure 3-9). This is an effect of how the downhole shaft turbine pump was modeled in this simulation; the wellhead back-pressure was fixed, and the production rate controlled, by setting a fixed mass flow rate at down hole (e.g., top of the liner). However, in reality the pump had only one speed and the production rate was controlled by adjusting the back pressure at the wellhead (Miller and Vasquez, 1988). Therefore, the above mentioned undershot may not occur.

Figure 3-9: Energy Flow Rate During Variable Production

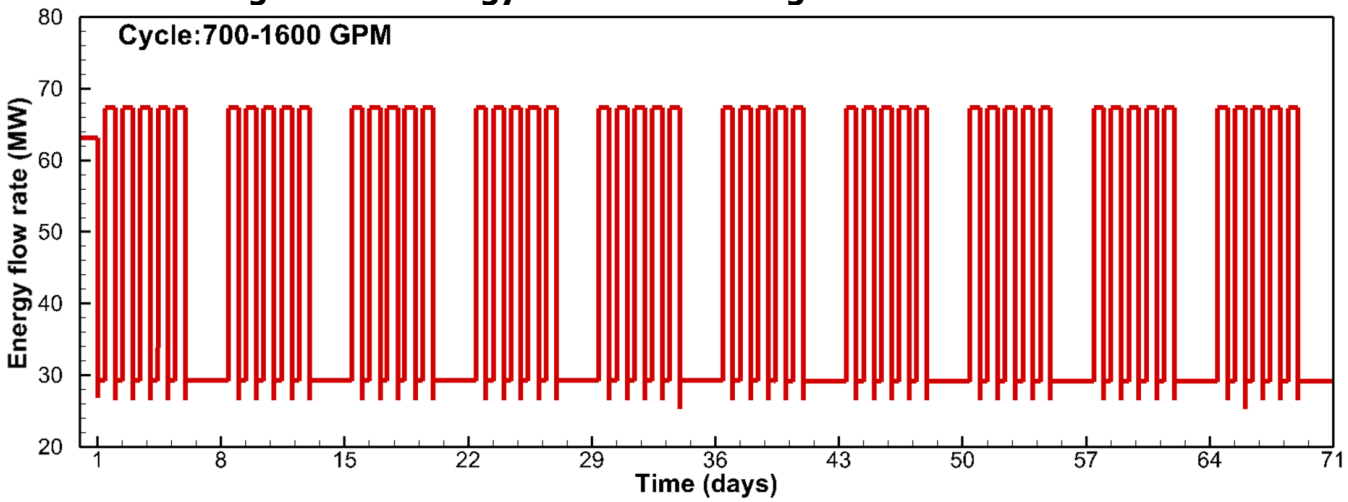

Calculated energy flow rate for an assumed cyclic production with production rates varied between 700 and 1600 GPM.

Source: LBNL

The bottom-hole pressure responded to cyclic production though the magnitude was small (less than 1 bar), while the wellhead pressure changed little due to the fixed back pressure (Figure 3-10a). Temperature in the well showed about a 1.6°C variation between peak and off-peak production, while the bottom-hole temperature was almost constant (Figure 3-10b). Pressure and temperature conditions indicate that single-phase liquid conditions are maintained in the well during variable production in this system (downhole shaft turbine pump with back pressure at the wellhead outlet). These small changes in pressure and temperature along the well can be attributed to the nearly uniform temperature of the well assembly and its surrounding rock along the well at the end of the 100-day constant-rate production (Figure 3-8a). The uniform temperature is close to the reservoir temperature of 352.4°F (178°C). During the cyclic production, there was little heat exchange between hot water in the wellbore and well assembly and the surrounding rock during the peak and off-peak periods.

Figure 3-10: Variable Production Pressure and Temperature Evolution

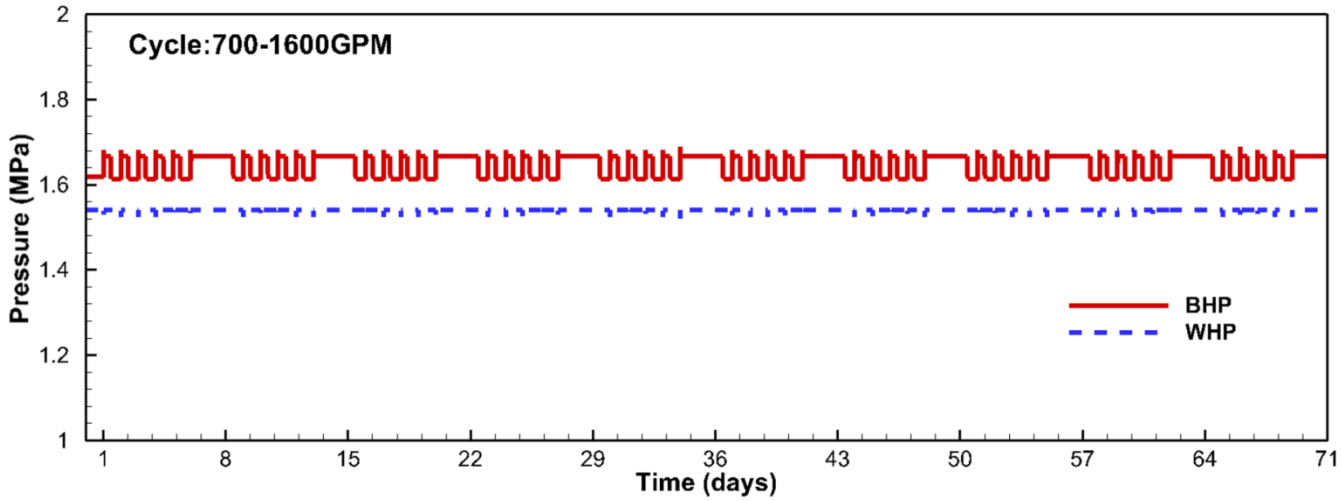

(a)

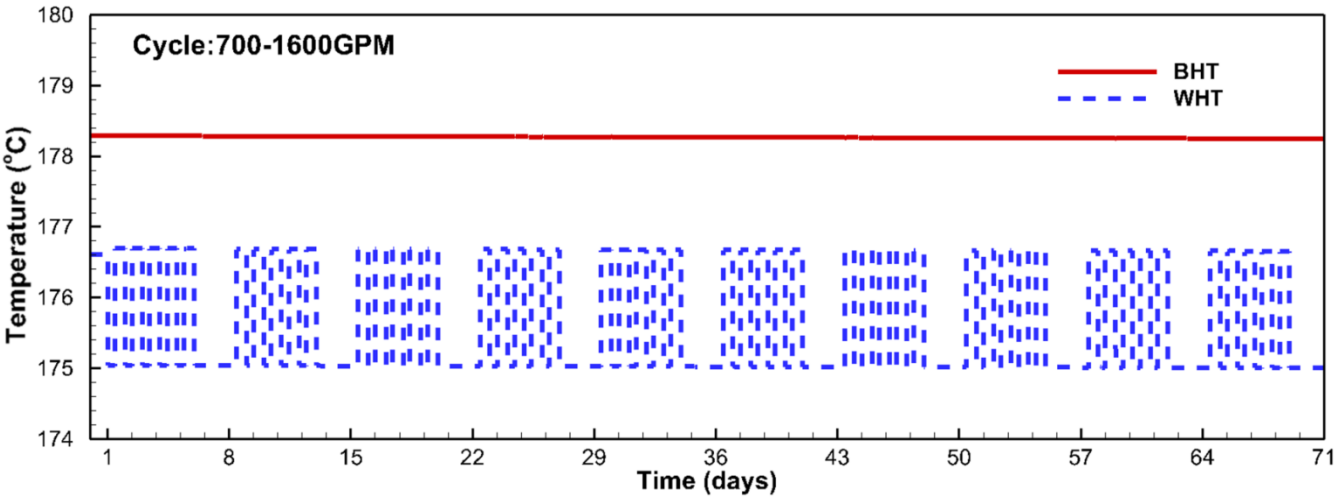

(b)

Simulation results for an assumed cyclic production with production rates varied between 700 and 1600 GPM; (a) Bottom-hole pressure (BHP) and wellhead pressure (WHP) and (b) Bottom-hole temperature (BHT) and wellhead temperature (WHT).

Source: LBNL

Both temperatures and pressures in the casing cement changed little in response to variable production (Figure 3-11). The pressure at the MidCement point was still very high, though it slowly decreased with time because of the very low permeability of cement (2×10^{-18} m^2 used in this model), which caused slow pressure dissipation in the middle of the cement.

Figure 3-11: Variable Production Pressure and Temperature in Cement

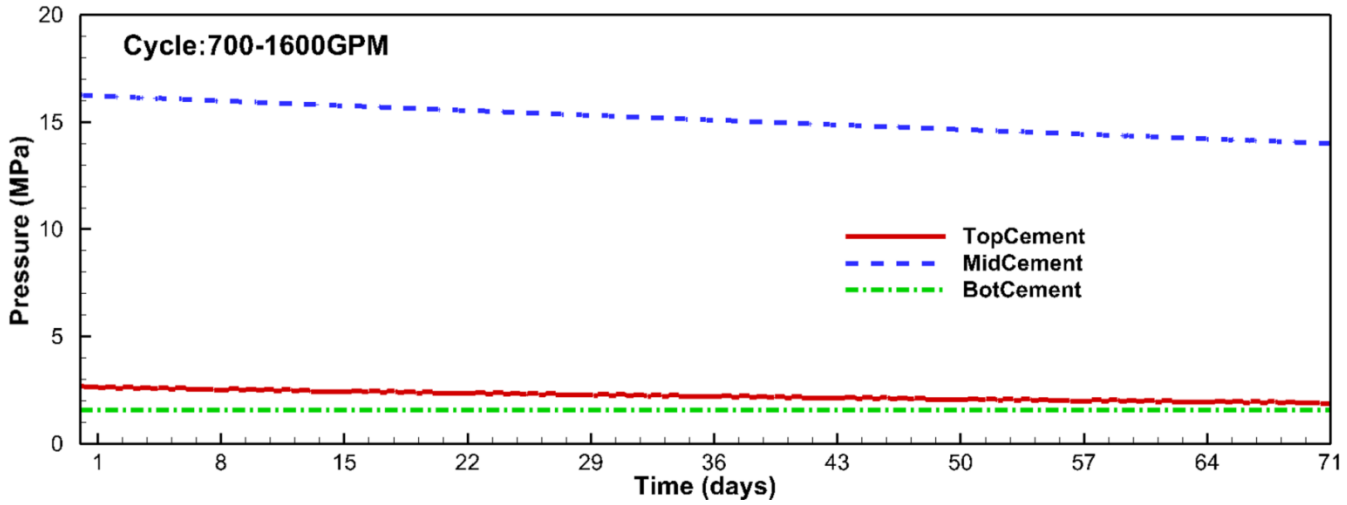

(a)

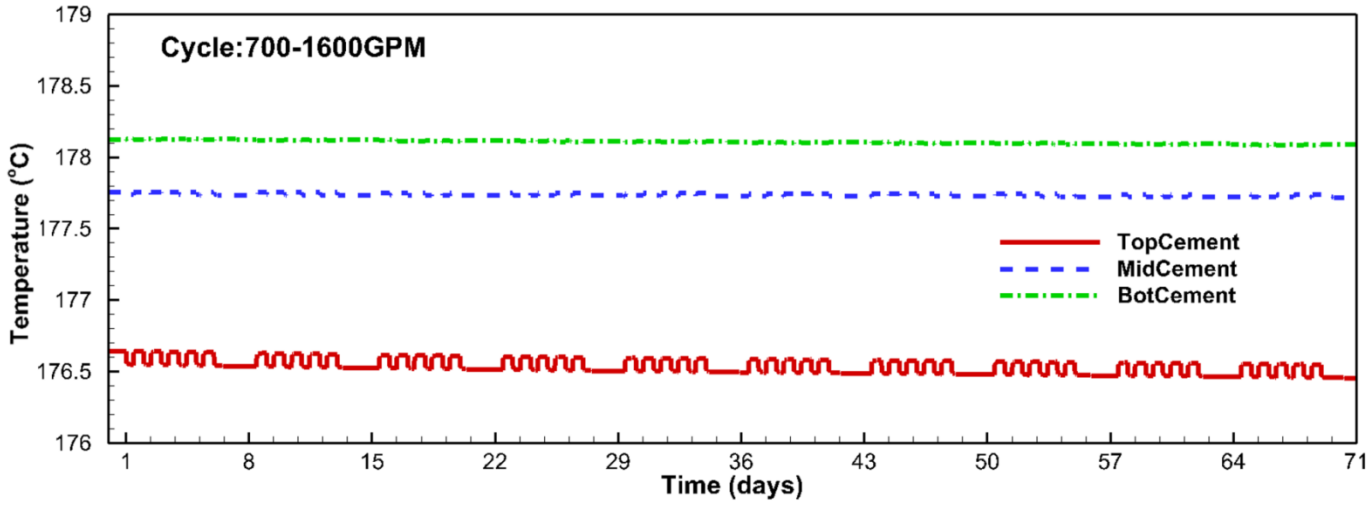

(b)

Calculated pressure and temperature evolution in the cement for an assumed cyclic production with production rates varied between 700 and 1600 GPM; (a) pressure and (b) temperature. TopCement, MidCement and BotCement output locations within the cemented portions of the well completion are shown in Figure 3-7.

Source: LBNL

Summary of T2WELL Analysis and Implications for Well Integrity Analysis

This section provides a summary of the T2WELL analysis for both steam- and liquid dominated systems and implications for the well integrity analysis.

For a steam-dominated geothermal system, the T2WELL analysis of coupled reservoir-wellbore processes showed that the highest thermal perturbation, ΔT, caused by constant-rate production, occurred in the shallow formations beneath the ground surface and near the production wellbore. In this zone (with the lowest initial temperature) temperature increased quickly with production as the temperature difference between the initial temperature and hot-

water temperature in the well is the largest. Produced hot water continuously heats the well assembly and surrounding rock, leading to a relatively uniform temperature profile along the well depth and a ΔT decreasing with depth. In the case of production from a deep geothermal well, similar to that of the P25 production well at the northwest Geysers, a maximum temperature increase of ΔT ≈ 195°C was calculated. At the end of the constant-rate production over 100 days, the temperature variation along the well is less than 35°C, significantly smaller than the initial variation of 180°C that is based on the thermal gradient. These temperature increases during initial start-up of the production are the highest in the case of production from a deep and hot geothermal system, such as the steam-dominated system at The Geysers.

In the case of a shallow liquid-dominated geothermal system, similar to that at the Casa Diablo, a maximum temperature increase ΔT ≈ 55°C was calculated. At the end of the constant-rate production over 100 days, the temperature variation with depth is very small, less than 2°C, indicating that the well assembly and surrounding rock have a uniformly distributed temperature.

Another important observation potentially relevant for well integrity is the significant increase in pore-fluid pressure within the cement sheath behind the steel casing. These pressure increases were caused by thermal-pressurization from a larger thermal expansion coefficient of water in the cement than the cement itself. The highest pressure increase was 60 MPa for the steam-dominated case and 30 MPa for the liquid-dominated case, all very high during the most dramatic temperature increase in constant-rate production. At the end of this period, the pressure increases decayed to less than 5 MPa in both cases since the temperature in the well assembly was relatively stable.

For the subsequent flexible-mode production, the magnitude of temperature changes with daily production cycles depended upon the temperature profile along the well at the end of the constant-rate production. If the temperature is uniform with the reservoir temperature, there are no temperature changes during the cycles because no heat exchange occurs between produced hot steam/water and the well assembly and surrounding rock. In the case of a deep steam-dominated system, the largest fluctuations in shallow wellbore temperature and pressure occurred, with pressure fluctuations on the order of about 1.5 MPa and temperature changes of about 5°C. In the case of a liquid-dominated system, the temperature and pressure changes were so small that they could be considered insignificant for well integrity. This is for the assumed cases of reducing production to about 40 percent during off-peak production cycles. However, in a sensitivity study with complete shut-ins in each cycle for the same Casa Diablo system, the maximum temperature changes between peak and off-peak cycles can reach 30°C at the wellhead (Rutqvist et al., 2020a). These temperature changes could induce more significant stress changes. This shows the importance of the design of the production cycling since keeping some hot fluid flowing can significantly reduce the potential impact of flexible production (Rutqvist et al., 2020a).

There are several implications for well integrity analysis:

- The potential highest impact on well integrity would likely occur at the shallowest part of the well assembly where temperature changes are highest for both liquid- and steam-dominated geothermal systems.

- The highest potential impact on well integrity occurred in the early startup of production after a longer curtailment, because of rapid increases in temperature with associated thermal pressurization in the cement behind the steel casing.
- During variable production with daily cycles, the temperature and pressure fluctuations were highest for production from deep and hot systems, such as the steam-dominated system considered in this study.
- On the basis of these results, the well integrity analysis presented in the next section focused on the initial startup for both shallow and deep wells, whereas cyclic changes were only investigated for a steam-dominated case.

In the thermal-hydraulic analysis using T2WELL, an initial startup period of 100 days was used before a cyclic production period of 100 days. This represents the case for an existing production well to switch from current constant-rate production to flexible-mode production. For a new production well, there is no such initial startup period, and cyclic production starts from the beginning. In this case, significant transient changes in pressure and temperature in the well assembly were expected.

Mechanical Analysis Due to Temperature and Pressure Responses

Coupled multiphase flow, heat transport and mechanical modeling were conducted using T2WELL-FLAC3D, with the mechanical component focused on some of the vulnerable parts of the well assembly, namely its shallowest part.

Coupled Flow and Geomechanical Model Setup

Figure 3-12 shows a 3D mechanical model of the well assembly for the deep geothermal well in the steam-dominated reservoir (P25 at The Geysers) and how it is linked to the larger scale T2WELL simulation model. The T2WELL simulations were conducted using an axisymmetric model domain, but the T2WELL-FLAC3D coupled THM analysis was conducted on co-located numerical grid elements. This means that the pressure and temperature evolution calculated in T2WELL at a depth of 2.4 m was imported into the mechanical analysis along the radius of the 3D model. The main reason for adopting a 3D model in the mechanical analysis was that anisotropic horizontal in situ stress could be an important consideration. In this particular case at 2.4 m depth, the in-situ stresses were very small; there was not much of a mechanical force from the surrounding formations on the well assembly at this depth. The mechanical model included components of host rock, cement, and casings as well as slip interfaces between these components. These slip interfaces allowed for frictional failure using Coulomb criterion as well as elastic opening of the interfaces caused by tensile failure.

Figure 3-12: Coupled T2WELL and FLAC3D Models

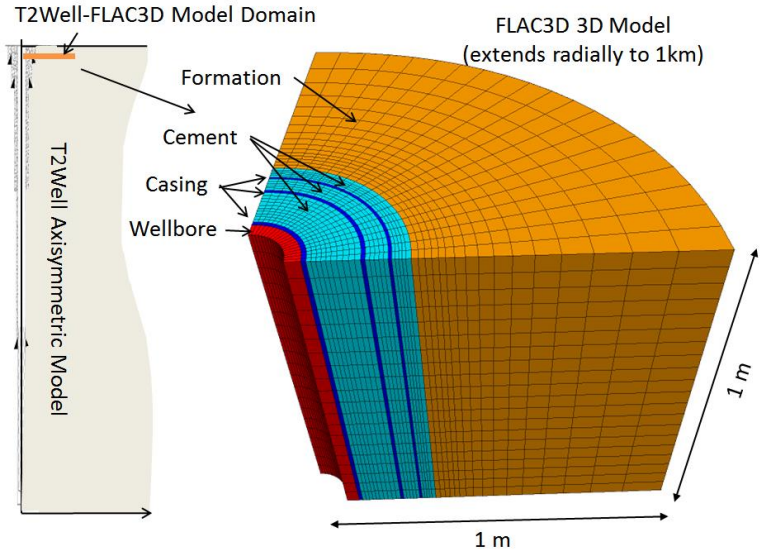

Coupled T2WELL and FLAC3D model domains, including T2WELL large-scale axial symmetric model domain and FLAC3D mechanical model domain of the shallowest part of the production well.

Source: LBNL

Figure 3-13 shows the FLAC3D model geometry for the two types of wells considered in this study, shown in Figures 3-3 and 3-7. Both types of wells have a well assembly consisting of multiple steel casings and cement sheaths, but the dimensions of the well completions were different which impacted the coupled THM evolution. The team simulated mechanical responses considering the elasto-plastic properties of the cement, rock, and frictional interfaces. Researchers applied elasto-plastic Mohr-Coulomb properties taken from the literature regarding the cement and host rocks (Rutqvist et al., 2018b; 2020a). These properties are reasonable and the team is also continuously updating the properties based on site-specific data.

Figure 3-13: FLAC3D Well Models

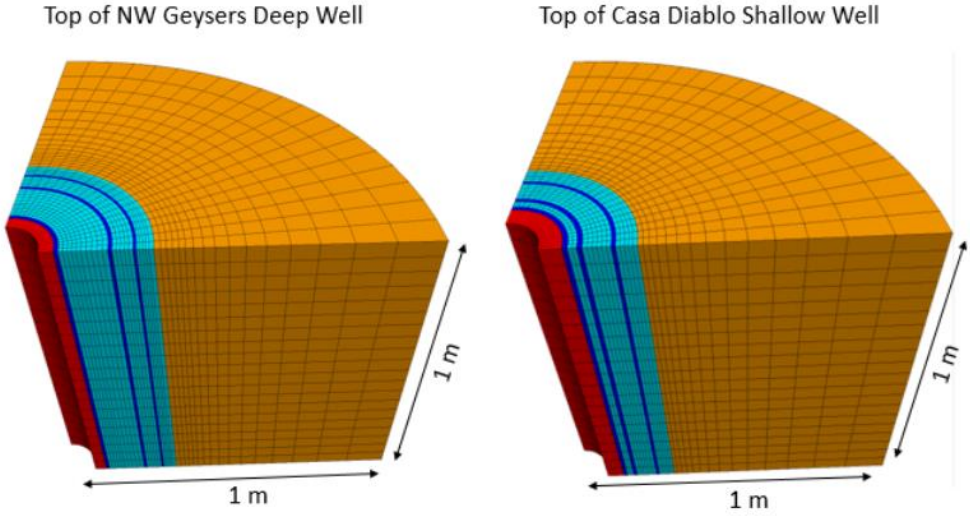

FLAC3D mechanical model domains of the shallowest part of the production wells at (a) NW Geysers P25 deep geothermal well and (b) Casa Diablo shallow geothermal well.

Deep Steam-Dominated System

Figure 3-14 shows how temperature and pressure increased very rapidly in the cement behind the innermost casing, as well as between the two outermost casings. The temperature and pressure changes were very high in the cement behind the innermost casing, while changes were smaller but still very high between the two outermost casings.

Figure 3-14: Temperature and Pressure in Cement

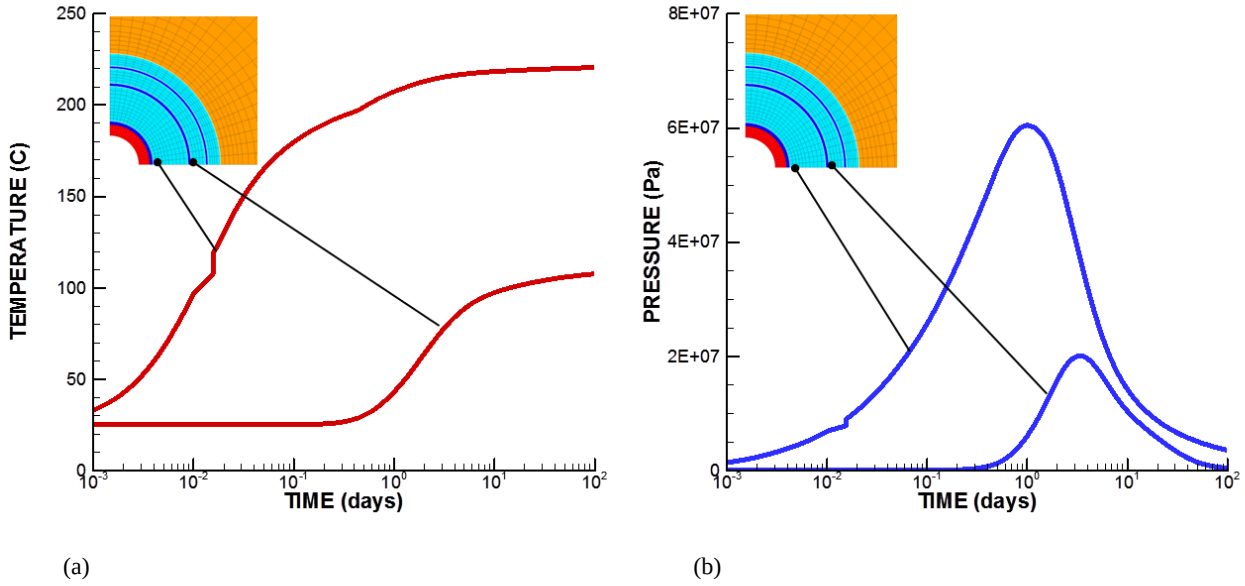

(a) (b)

Calculated (a) temperature and (b) pressure evolutions in two cement sections at the shallow part of the production well (production from a deep geothermal well).

Source: LBNL

Figure 3-15 shows the stress path (maximum compressive versus minimum compressive stresses) in the second cement section, along with the Mohr-Coulomb failure envelope. The stress evolution was very complex, with both tensile and shear yielding occurring during the first few days of production. Thereafter, the principal stresses moved away from the failure line as a result of increasing thermal stress that provides an increasing confining stress. Finally, at pseudo-steady conditions at 100 days, the stresses reached a more uniform state of 13 to 18 MPa effective stress.

Figure 3-15: Stress Path in Cement

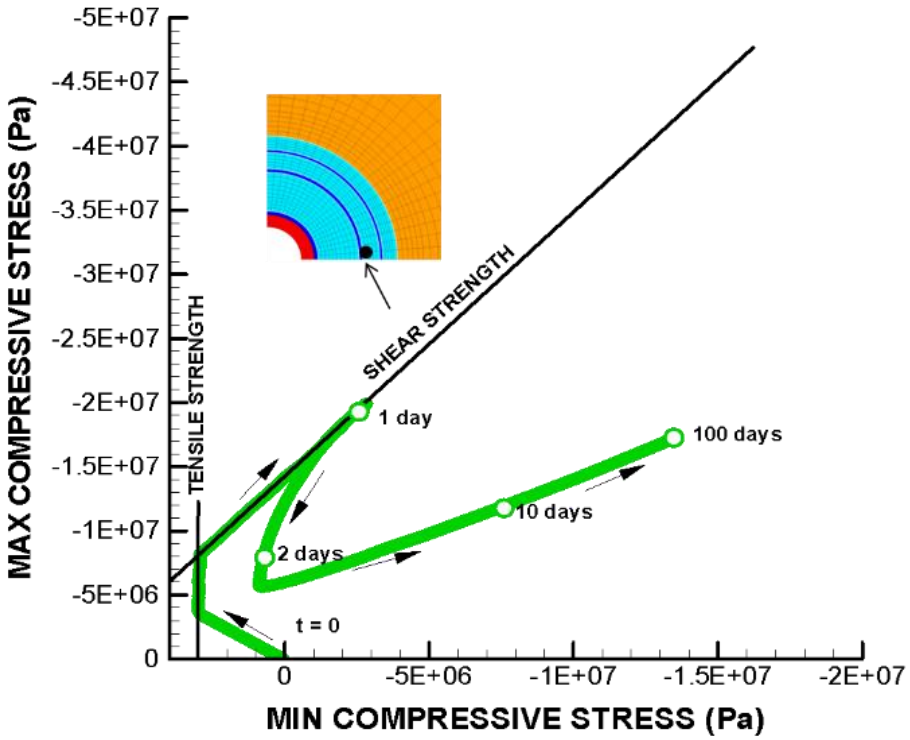

Effective stress path for one location in the 2nd cement section.

Source: LBNL

High tangential stresses also built up in the steel casing, with high compression in the innermost casing and tensile stresses in the two outermost casings (Figure 3-16). The high compressive stresses in the innermost steel casing are a direct effect of thermal expansion of a stiff material that when confined will lead to high thermal stress. The high tensile stress built up in the two outer casings is a result of the general thermal expansion of the cement in the inner parts of the well assembly that causes displacement and high stress on the outermost steel casings. The stress increases as high as 800 MPa, which could likely lead to yielding depending on the grade of the steel material. Yielding was not accounted for in the current analysis, but could be included in future analysis.

For the simulation of variable production we previously concluded that for cyclic production with curtailment down to 40 percent, some pressure and temperature changes occur in the case of a steam-dominated geothermal well, while changes are negligible for a liquid-dominated geothermal system. For the steam-dominated system, the simulation of variable production resulted in both temperature and pressure variations in the cement, with the highest magnitudes in the innermost cement. With daily production variations, the temperature fluctuates with a magnitude of about 5°C and the pressure with a magnitude of about 1.5 MPa (Figure 3-17a). These changes in turn result in stress cycles with magnitudes of about 1 MPa in the cement (Figure 3-17b). These changes in stress are small compared to the stress changes that occurred during the preceding start-up and 100 days of steady production. Obviously, the stress change that could occur during variable production will very much depend on the schedule and magnitudes of the production cycles.

Figure 3-16: Casing Stress

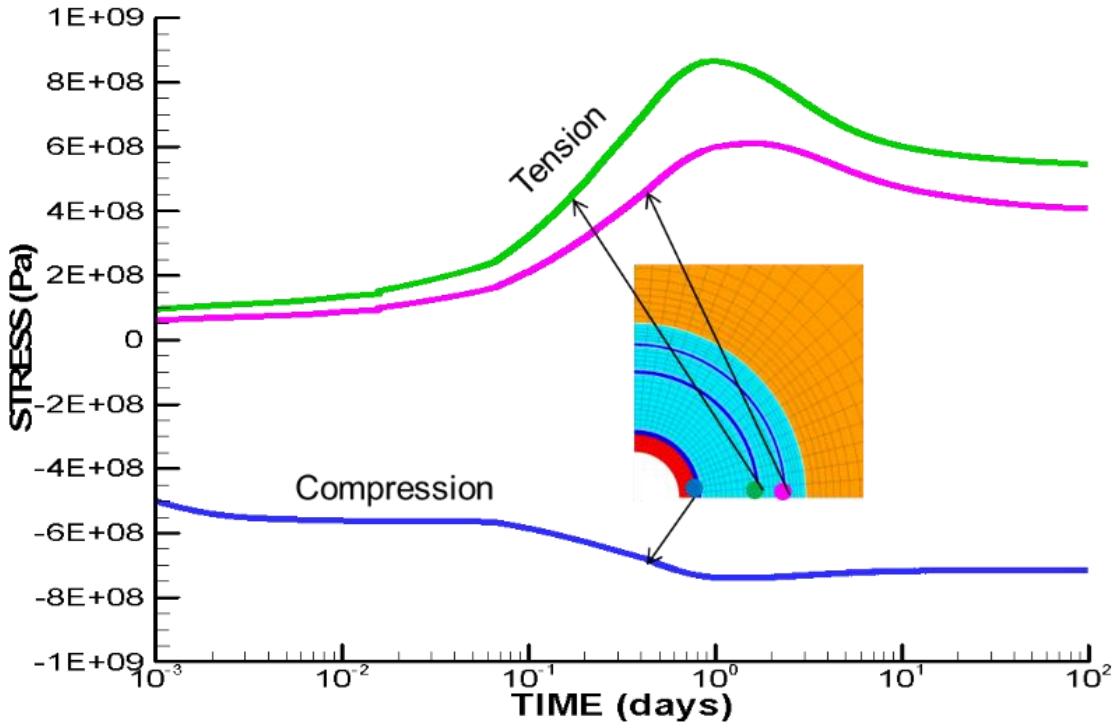

Calculated tangential stress evolution in all 3 casings in the shallowest part of the well.

Source: LBNL

Figure 3-17: Temperature, Pressure and Stress During Variable Production

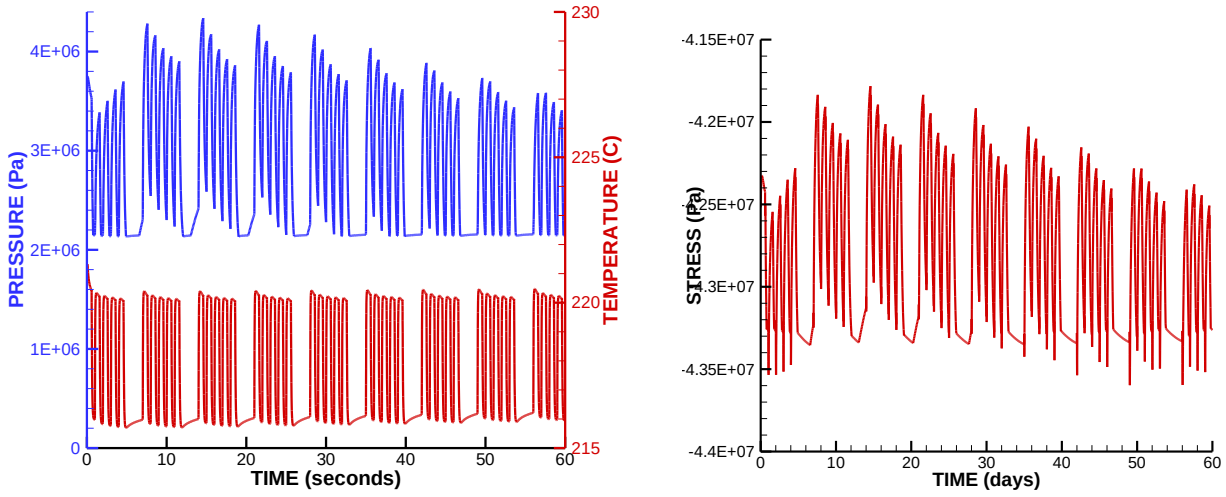

(a) (b)

Calculated variable production evolution in (a) pressure and temperature and (b) stress in the cement behind the innermost casing.

Source: LBNL

Shallow Liquid-Dominated Systems

For production from the shallow geothermal well, the simulation also shows that failure in the cement behind casing could occur at an early stage during production start-up. As observed in Figure 3-18, the temperature and pressure increase very rapidly in the cement behind the innermost casing as well as between the two outermost casings. However, in this case the relative changes in temperature and pressure are smaller as the initial temperature is much higher. It should be said that the estimate of temperature in the well assembly near the surface might have been overestimated due to lack of data in the region when doing the initial model calibration. Thus, it should be important to characterize the near surface temperature in the well system.

Figure 3-18: Temperature and Pressure in Cement

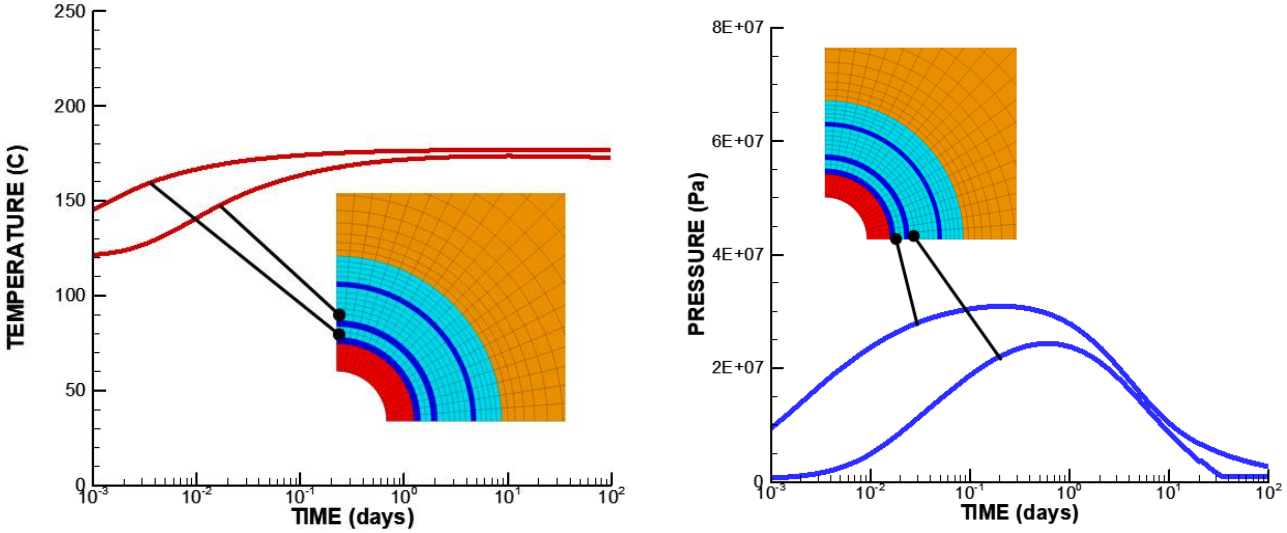

(a) (b)

Calculated (a) temperature and (b) pressure evolutions in two cement sections at the shallow part of the production well (production from a shallow geothermal well).

Source: LBNL

Figure 3-19 shows the stress path (maximum compressive versus minimum compressive stresses) at the same two locations, along with the Mohr-Coulomb failure envelope. The stress evolution is complex, with tensile failure occurring within one day of production. Thereafter, the principal stresses moved away from the failure line as a result of increasing thermal stress that provided an increasing confining stress.

Figure 3-19: Stress Path in Cement

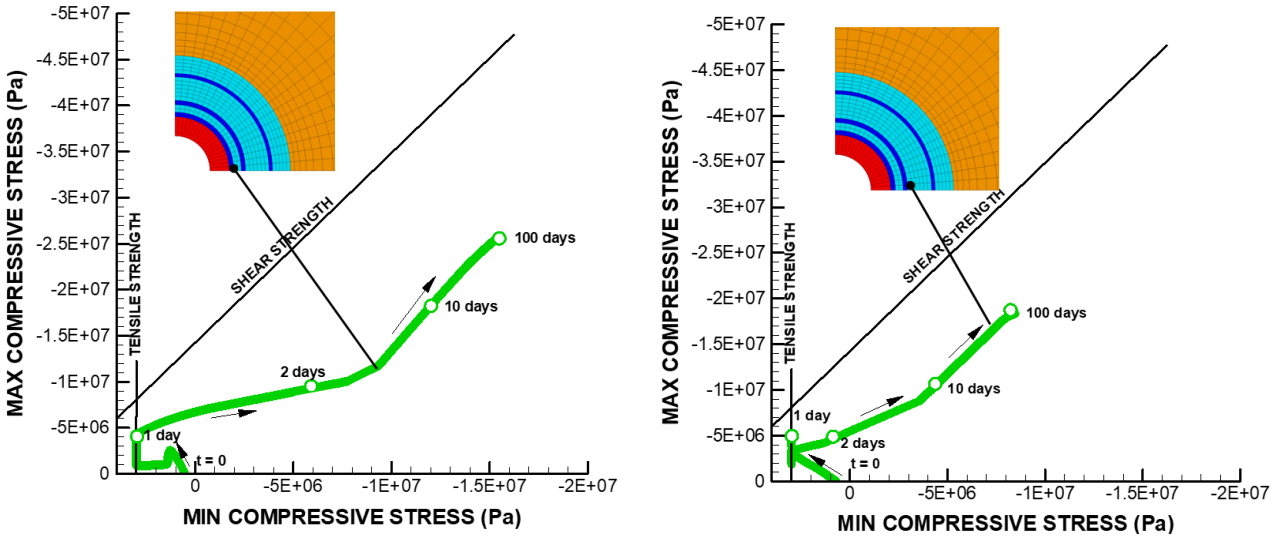

Effective stress path for one location in (a) first cement section and (b) second cement section.

Source: LBNL

High tangential stresses also built up in the steel casing, with high compression in the innermost casing and tensile stresses in the two outermost casings (Figure 3-20). Peak tensile and compressive stresses were smaller than in the case of production from a deep well (compare stress evolution in Figures 3-16 and 3-20). The tangential stress changes were smaller because the temperature changes and subsequent thermal stresses were smaller in this case. Nevertheless, stress increases as high as 400 MPa could still lead to yielding depending on the grade of the steel.

Figure 3-20: Casing Stress

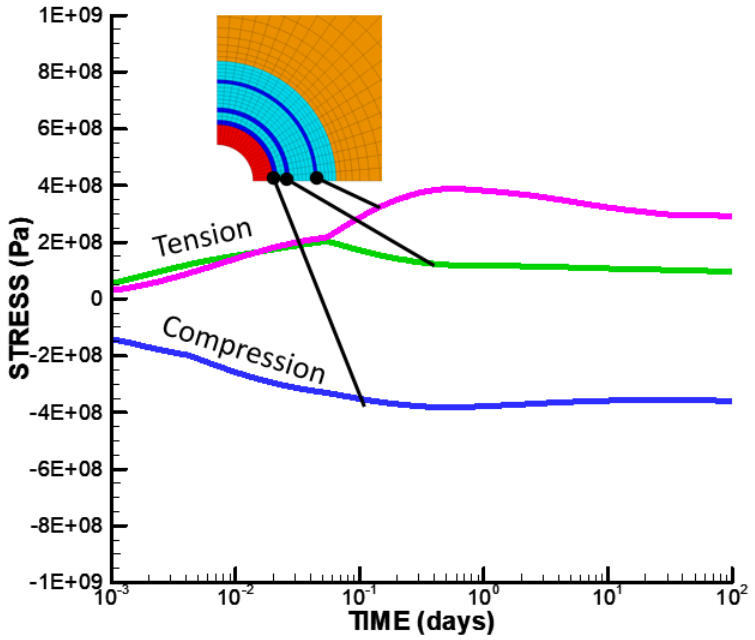

Calculated tangential stress evolution in all 3 casings in the shallowest part of the well.

Source: LBNL

Variable production for the liquid dominated system at the Casa Diablo well did not result in significant pressure and temperature changes when off-peak production was reduced to about 40 percent of the real production rate (Figure 13); no significant stress changes occurred due to variable production, so variable production would not impact mechanical well integrity for this shallow geothermal system.

Impact on Scaling and Corrosion

Mineral scaling is typically not an issue for a steam-dominated system such as The Geysers. However, pressure variations from a flexible production mode could affect vapor condensation and the scrubbing of acid gases such as HCl. This could possibly increase corrosion if condensation occurs in the well. Conversely, increased condensation by vapor adsorption on mineral surfaces and capillary condensation in small pores in rocks surrounding production wells could scavenge and neutralize HCl away from those wells and therefore lower their corrosion potential (e.g., Pruess et al., 2007). This study shows that under the flexible production mode considered here, increased vapor condensation within the well would not be expected; therefore, cyclic production should not be detrimental in terms of corrosion.

For the case of a liquid-dominated system such as Casa Diablo, the potential for mineral scaling was evaluated using the CHILLER simulations as presented in Rutqvist et al. (2019; 2020a). Fluid (water + gas) was first reconstructed. The reconstructed fluid shows near-equilibrium with several minerals reasonably expected at depth (rhyolitic formation) and temperatures (around 352.4°F [178°C]) consistent with deep temperatures recorded in well MBP-3, thus, increasing confidence in the results. Simulations of cooling without and with iso-enthalpic boiling were then performed with the reconstructed fluid composition to test

temperature and pressure regimes that could exacerbate mineral scaling or the acidity of the fluid, with the goal of constraining pressures and temperatures suitable for flexible production modes.

The final results show that under the current fixed production mode (with pressure maintained high enough to prevent boiling) and as long as the temperature is maintained above 158°F (70°C), limited scaling is expected, consisting primarily of Fe carbonates and hydroxides with minor clay, carbonates, and sulfides (corresponding to amounts up to about 5 kilograms (kg) of scale per day at 500 GPM (Figure 3-21). However, cooling the fluid below about 158°F (70°C) could result in the precipitation of significant amounts of amorphous silica corresponding to amounts up to ~400 kg per day at 500 GPM, although this would not be expected provided that temperatures at the heat exchanger were not lowered from the range currently in effect (greater than 185°F [85°C]).

Figure 3-21: Mineral Precipitation in Wells

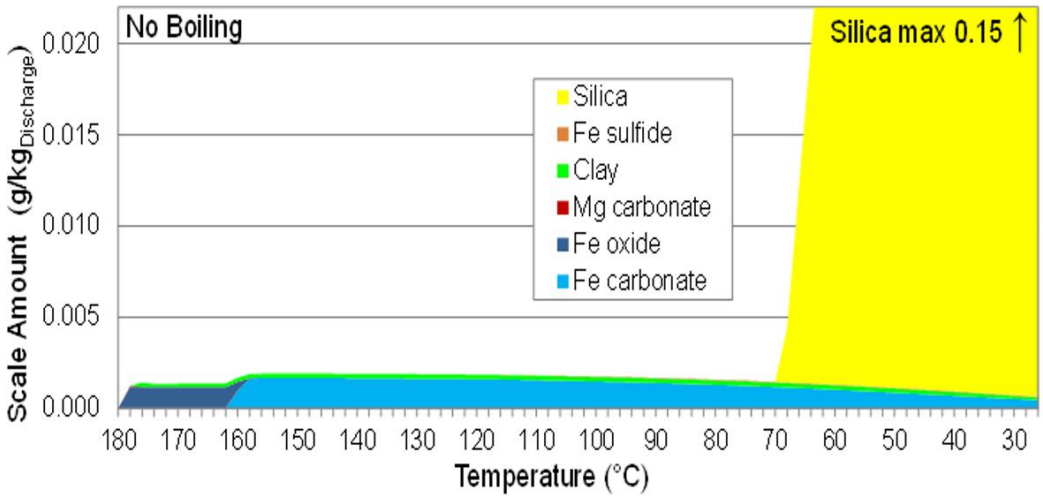

Simulations of cooling without boiling for a Casa Diablo geothermal fluid: computed amounts and types of deposited minerals.

Source: LBNL

For liquid-dominated systems, if boiling was allowed to occur in production wells (which is not the case at Casa Diablo), a flexible production schedule would be expected to result in smearing scale over a larger depth interval than with a fixed schedule. Boiling initiating at high temperatures would be expected to produce significantly more scaling than if pressure was controlled such that flashing was suppressed or occurred at lower temperatures, although in the case of intermediate temperature systems, the amount of scale deposited from boiling at different temperatures below about 356°F (180°C) should not differ appreciably. For these systems, as long as the wellhead pressure is maintained above saturation pressure and the temperature maintained above silica saturation temperatures (about 158°F [70°C] at Casa Diablo), a flexible production mode would not be expected to affect scaling or corrosion more than under a fixed schedule.

Impact on Reservoir Behavior

Heat transport in a geothermal reservoir in response to cold-water injection and hot-water production was simulated using the SHPALib code developed in this study (Zhou et al., 2017a,

b, 2019). The modeling focused on (1) fracture-matrix heat exchange as a function of different shapes and sizes of matrix blocks, (2) heat transport in fractured reservoirs under linear and radial flow with fracture-matrix heat exchange accurately accounted for, and (3) heat transport in fracture zones imbedded in the rock matrix. These modeling scenarios focused on constant-rate fluid injection or flow. It is well-known that constant-rate production only directly affects fluid flow, which in turn affects long-term heat transport, rather than short-time rate perturbations. The reservoir temperature near a production well is not directly affected by hot-water production, as shown by the bottomhole temperature in the reservoir-wellbore thermal-hydraulic analysis described previously. It is expected that flexible-mode production with variable rates does not affect reservoir temperature near the production well within the 100-day time scale of this study. Heat-transport modeling was therefore conducted to evaluate the impact of cold-water injection on reservoir behavior.

Fracture-Matrix Heat Exchange

Fracture-matrix heat exchange was investigated by developing a simple, approximate solution consisting of an early-time error-function-type solution and a late-time exponential-type solution. This general solution is valid for all regular shapes of matrix blocks (e.g., slab, square, cube, rectangle, rectangular parallelepipeds, cylinder, or sphere). Figure 3-22 shows the general solution of dimensionless average temperatures of matrix blocks under fixed surface conditions with a unity temperature change. This indicates that the solution accurately captures the transient heat exchange from the initial condition ($T_d = 0$) to the equilibrium condition ($T_d = 1$).

Figure 3-22: Fracture-Matrix Heat Exchange Solution

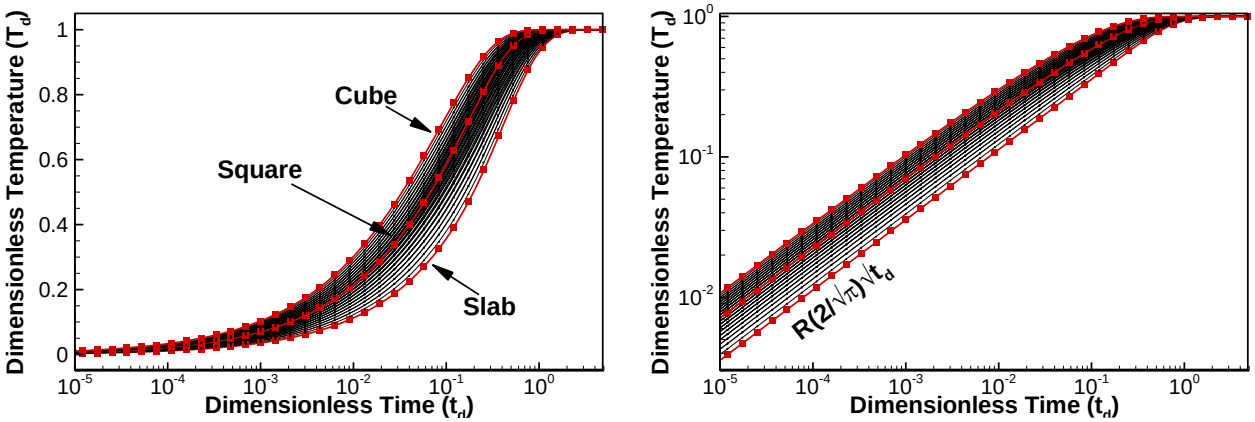

Approximate solution of fracture-matrix heat exchange for regular matrix-block shapes: slab, square, cube, rectangle, and rectangular parallelepiped: comparison between the developed approximate solution (in symbols) and very complex exact solutions (in lines).

Source: LBNL

Figure 3-23 shows the distribution of dimensionless temperature as functions of isotropic block shapes (e.g., slab, cylinder, and sphere), 2-D rectangles with aspect ratio R_{l1}, and 3-D rectangular parallelepipeds with aspect ratios R_{l1} and R_{l2}, as well as dimensionless time t_d. This simple analytical solution is significantly more computationally efficient than traditional solutions, while maintaining high accuracy. This solution of spatially distributed dimensionless temperature is consistent with average dimensionless temperature, which can be directly used for calculating heat exchange flux.

Figure 3-23: Fracture-Matrix Exchange Solution: Temperature Distribution

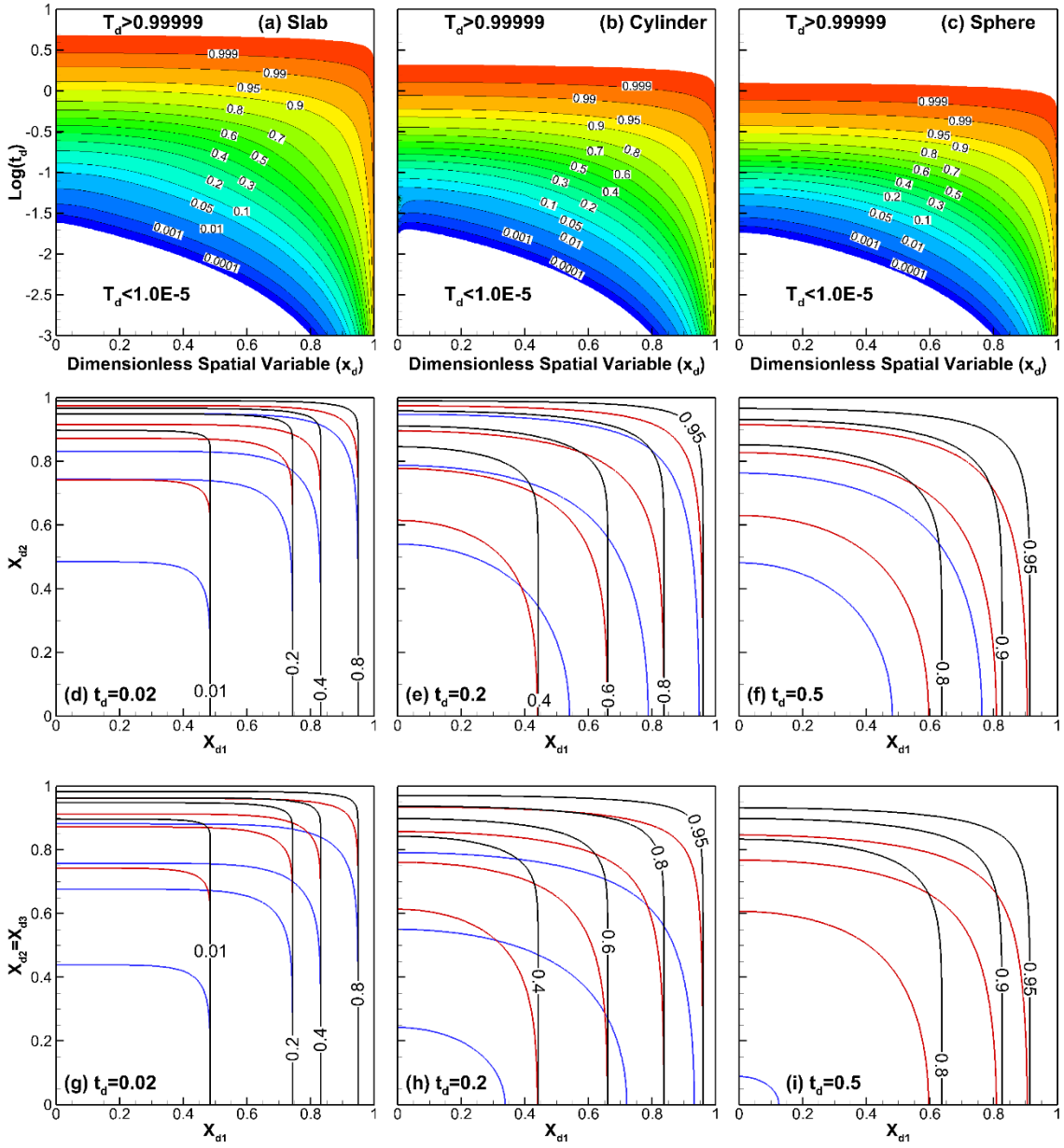

(a-c) Contour of dimensionless temperature (T_d) over the domain ($x_d, \log t_d$) for isotropic blocks (slab, cylinder, and sphere), (d-f) T_d contour over 2D rectangles (x_{d1}, x_{d2}) at $t_d = 0.02, 0.2, 0.5$, and (g-i) T_d contour over 3D rectangular parallelepipeds (x_{d1}, x_{d2}) with $x_{d3} = x_{d2}$ at $t_d = 0.02, 0.2, 0.5$. Note that the contour lines and their labels for the three rectangles with $R_{l2} = 1.0$ (in blue lines), 0.5 (in red), and 0.2 (in black) and the three parallelepipeds with $(R_{l1}, R_{l2}) =$ (1.0, 1.0) (in blue), (0.5, 0.2) (in red), and (0.2, 0.1) (in black).

Source: LBNL

The developed approximate solutions were also compared with the conventional dual-porosity model implemented in the TOUGH family of codes (Pruess et al., 1999). Figure 3-24 shows that the dual porosity model predicts early-time heat flux in the form of $T_d \propto t_d$ while the approximate solution predicts that in the form of $T_d \propto \sqrt{t_d}$, with the coefficients dependent on the shape and aspect ratios of matrix blocks. This indicates that the convectional dual-porosity model underestimates heat flux before thermal equilibrium is reached between fractures and matrix blocks.

Figure 3-24: Comparison Between Approximate and Dual-Porosity Solutions

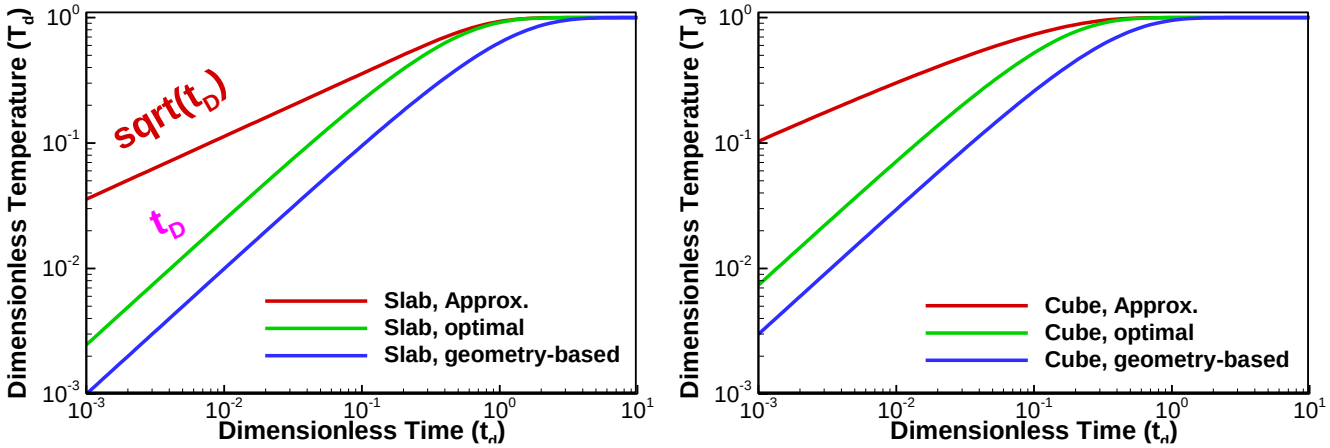

The approximate solution of heat flux (i.e., dimensionless temperature T_d) compared with convectional dual-porosity model with optimal or geometry-based coefficient.

Source: LBNL

Heat Transport in Fractured Geothermal Reservoirs

Modeling heat transport in fractured geothermal reservoirs was conducted to investigate convection-dispersion in fractures coupled with conduction in matrix blocks. To better understand this coupling, heat transport in single continuum (fractures or the rock matrix) was modeled separately. The volume fraction of fractures was 1 percent, while the volume fraction of matrix blocks was 99 percent. Figure 3-25 shows the temperature profiles along one dimension under the effect of different pore velocity and thermal dispersivity values.

Figure 3-25: Temperature Profiles for Single Continuum: Fractures or the Matrix

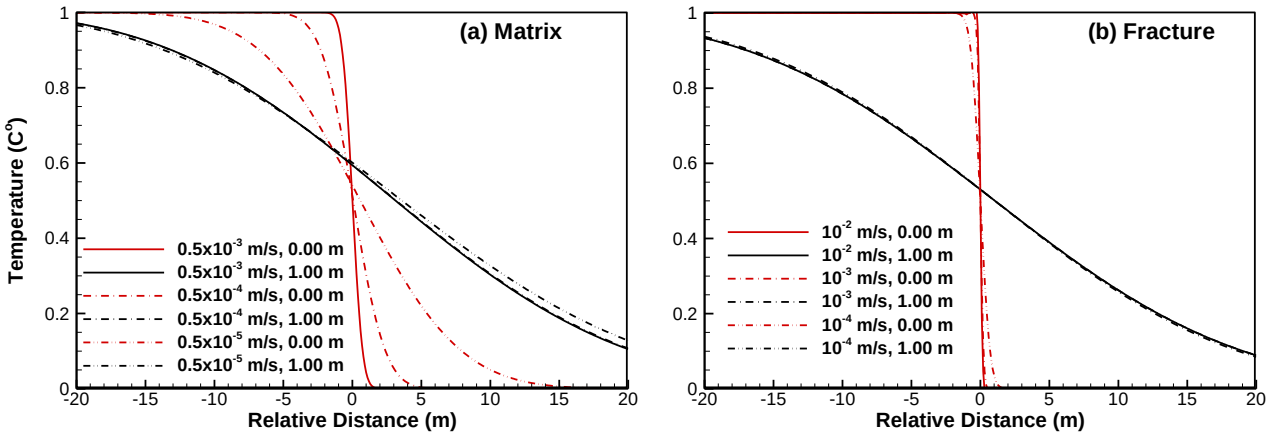

Heat-transport solutions under different pore velocity (in m/s) and thermal dispersivity (m) with temperature profiles centered at 23.87 m and 93.46 m for the matrix continuum and fracture continuum, respectively.

Source: LBNL

As shown in Figure 3-25, heat transport was slightly retarded in the fracture continuum with a porosity of 0.9 in comparison with the fluid travel distance of 100 m. Heat transport was significantly retarded in the matrix continuum with a porosity of 0.2 because the center (50 percent temperature) of the profile was located at 23.87 m. This significant retardation is attributed to heat storage in matrix solids, in addition to pore water. These comparisons

between heat transport in the fracture continuum, the matrix continuum, and fluid flow indicate that heat transport in the two continua is very different. For single fracture continuum, the temperature profile does not depend on pore velocity, but instead depends on thermal dispersivity. For the matrix continuum, the temperature profile depends on pore velocity for only very small dispersivity values.

For a fractured geothermal reservoir, heat transport in the fracture and matrix continua is coupled. In other words, heat convection-dispersion in the fracture continuum is coupled with heat conduction in the matrix continuum. Figure 3-26 shows the temperature profiles as functions of pore velocity and thermal dispersivity for the fracture continuum and the shapes and sizes of isotropic matrix blocks for the matrix continuum. Clearly pore velocity in the fracture continuum played a significant role in the shaping temperature profile. The higher the pore velocity is, the deeper the ΔT propagates. This effect is different for a single continuum because fracture-matrix heat exchange is a time-dependent process. Thermal dispersivity has a minor effect on temperature profile, which slightly increases thermal penetration because thermal dispersion leads to a dispersive profile, as shown in Figure 3-25. The complex interaction between dispersion, convection, and conduction was fully and accurately captured.

Figure 3-26: Temperature Profiles for a Fractured Reservoir With Isotropic Matrix Blocks

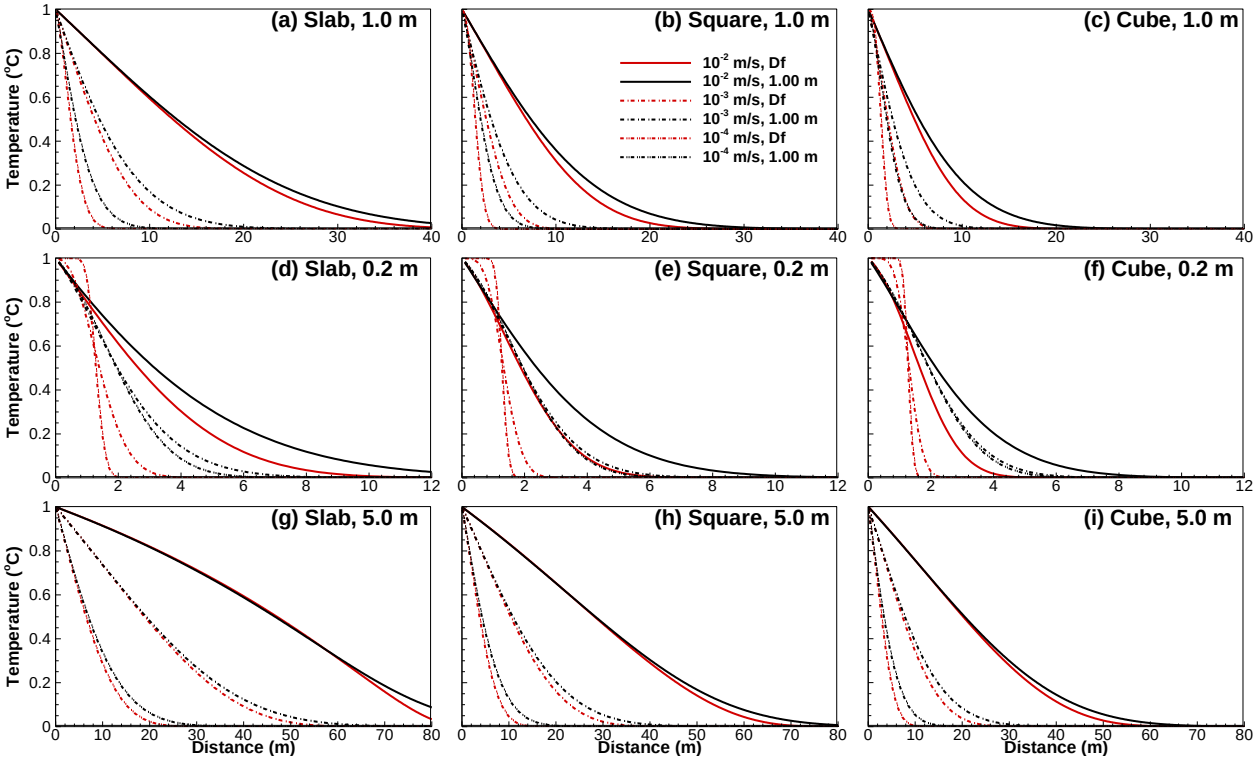

Temperature profiles as functions of isotropic matrix-block shapes (slab, sphere, and cube), pore velocity, and thermal dispersivity (1 m or 0 m with diffusivity only).

Source: LBNL

In addition to pore velocity and thermal dispersivity, the shape and size of matrix blocks also had significant effects on the temperature profile. The larger the length of a matrix block, the deeper the thermal penetration became. For a very small matrix block (0.2 m), thermal equilibrium between fractures and the matrix was possible within a short time, and the dual

continua act like a single continuum with a directly calculated retardation factor. For a large fracture spacing, the dual continua are not at thermal equilibrium, and heat exchange calculation is required. Heat exchange flux also depends on the shape of matrix blocks. Thermal penetration for slab-type matrix blocks was deeper than that for cube-type matrix blocks. For example, thermal breakthrough is at 100 m in the case of slab-type matrix blocks of 5.0 fracture spacing with a pore velocity of 0.01 m/s, even though breakthrough temperatures were small; in this case fluid and thermal breakthroughs were at the same time.

The aspect ratios of rectangular matrix blocks also affect temperature profiles because they affect heat exchange flux, as shown in Figure 3-22. Figure 3-27 shows the effects of aspect ratios on temperature profiles. The smaller the aspect ratios, the less heat exchange occurs, and the deeper the thermal penetration in the fracture continuum.

Figure 3-27: Temperature Profiles for a Fractured Reservoir With Rectangular Matrix Blocks

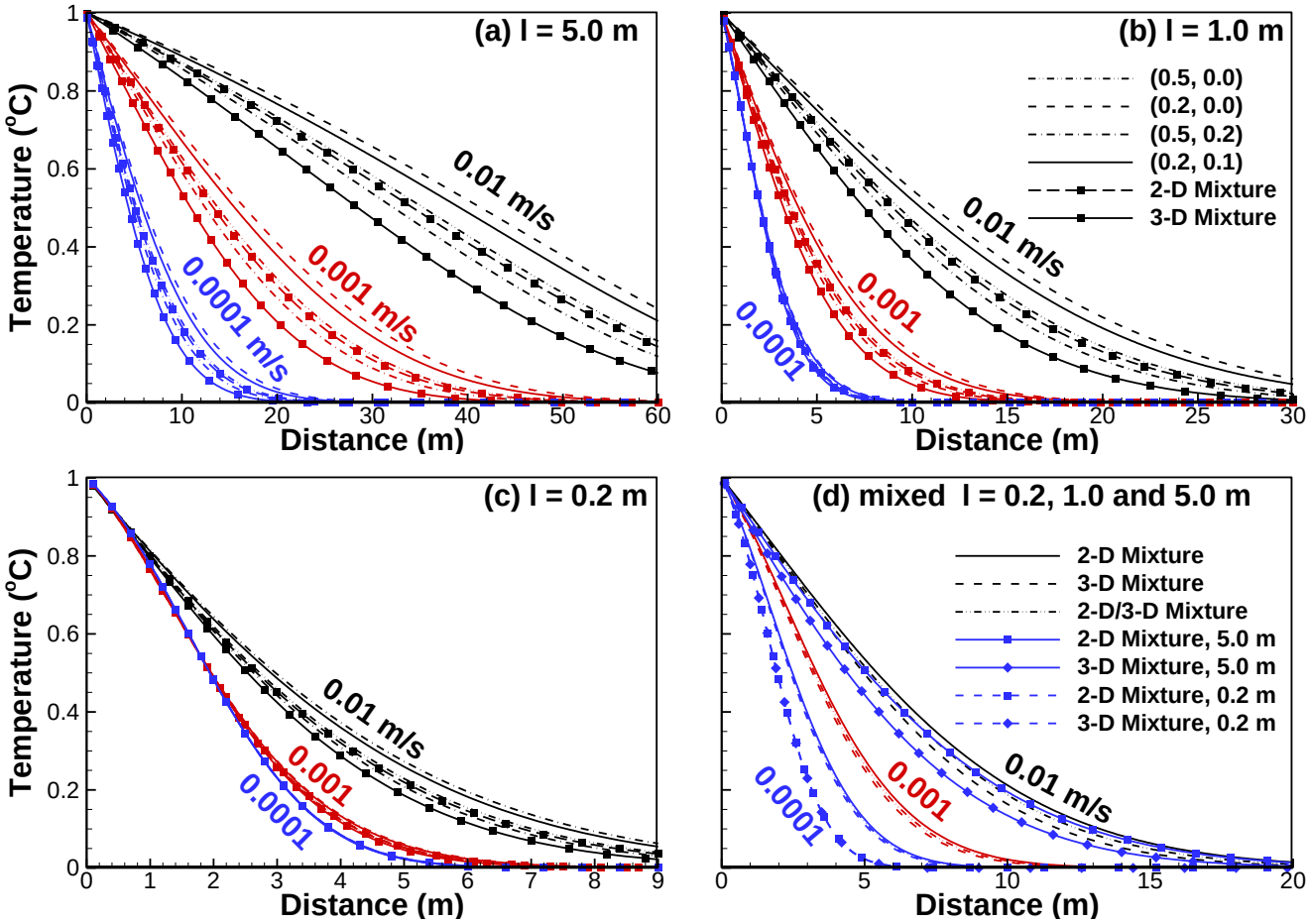

Heat-transport solutions under different pore velocity (in m/s) and thermal dispersivity in m with the temperature profiles centered at 23.87 m and 93.46 m for the matric continuum and fracture continuum, respectively.

Source: LBNL

For very small pore velocity, the time scale for heat exchange between matrix blocks and fractures is small; in this case, there is no further effect of matrix blocks' aspect ratios.

For a representative elementary volume (REV), there were many matrix blocks of different shapes and sizes (as well as aspect ratios). These matrix blocks were directly connected with fractures, and heat exchange between fractures and these matrix blocks occurred simultaneously. This type of effect is shown in Figure 3-27d for matrix blocks with fracture spacing of 0.2 m, 1.0 m, and 5.0 m. The combined effect resulted in temperature profiles between those of fracturing spacing of 0.2 m, 1.0 m, and 0.5 m.

In the studies described, heat transport modeling was conducted for linear flow with constant pore velocity in space, representing heat transport in linear fracture zones with matrix blocks. For cold-water injection, pore velocity may be of a radial flow nature and decreases with distance away from the injection well. Figure 3-28 shows temperature profiles as a function of radial distance from the injection well. The fluid travel distance was 100 m, at which point the Peclet number was 96.3, while travel time was 103.3 days.

Figure 3-28: Temperature Profiles for a Fractured Reservoir in Radial Flow

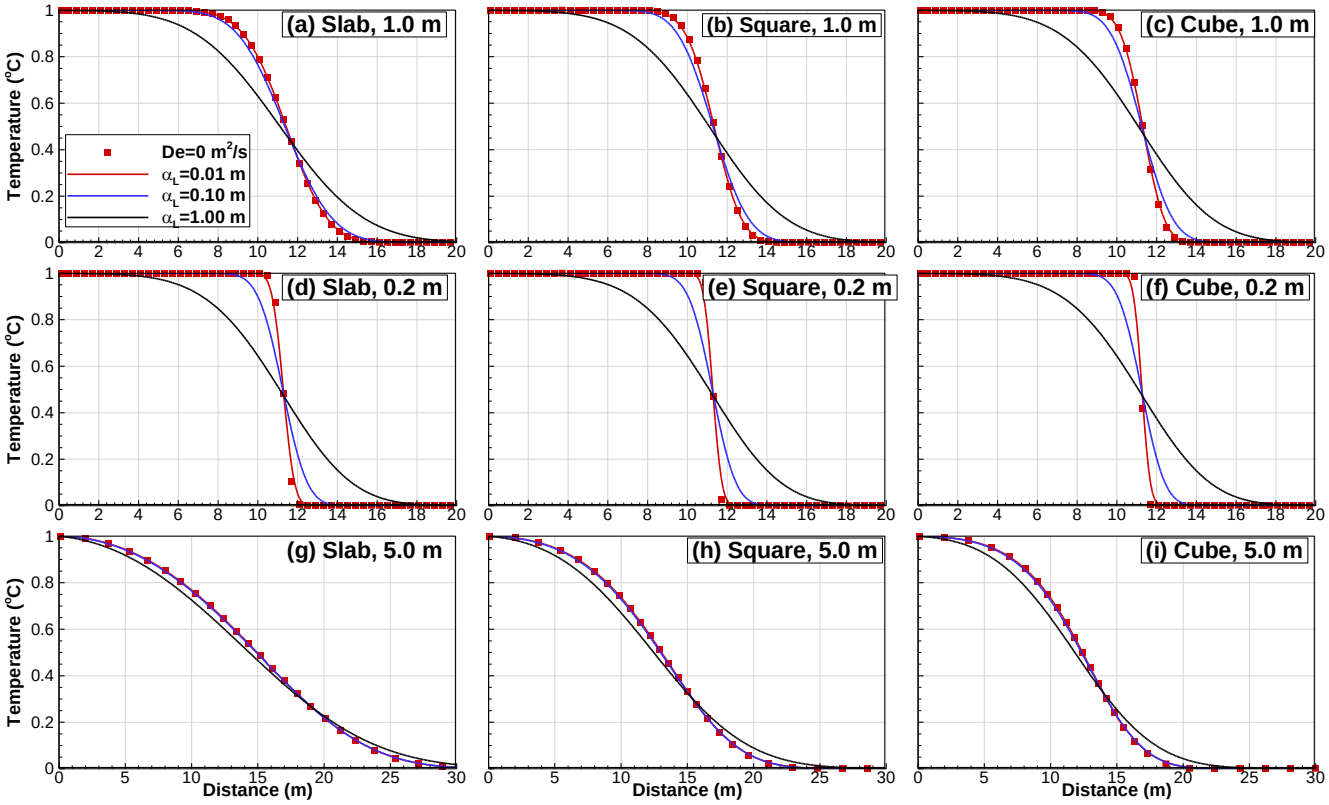

Temperature profiles with radial distance from an injection well, as functions of thermal dispersivity (α_L in m, or effective dispersion coefficient of 0) and shape (slab, square, and cube) and size (fracture spacing of 0.2, 1 and 5 m) of matrix blocks.

Source: LBNL

The maximum thermal penetration depth from the injection well was 30 m in the case of slab-type matrix blocks with fracture spacing of 5.0 m, while the minimum thermal penetration depth was 11.3 m for isotropic rectangular matrix blocks with fracture spacing of 0.2 m. This profile was sharp, with no effective dispersion coefficient, and the depth was directly calculated using a retardation factor of 78.62 (assuming the fracture and matrix continua were always at thermal equilibrium). Comparing temperature profiles for linear flow, the thermal

penetration depth was shorter in the radial flow field because of small pore velocity away from the injection well.

A geothermal reservoir is always bounded by low-permeability unfractured formations. In this case, there was heat exchange between the fractured reservoir and the unfractured aquitards. Figure 3-29 shows temperature profiles for the bounded fractured reservoir, with other conditions the same as shown in Figure 3-28. In the cases with or without thermal dispersion, temperature transport was further retarded by additional heat exchange with aquitards.

Figure 3-29: Temperature Profiles for an Aquitard-Bounded Fractured Reservoir in Radial Flow

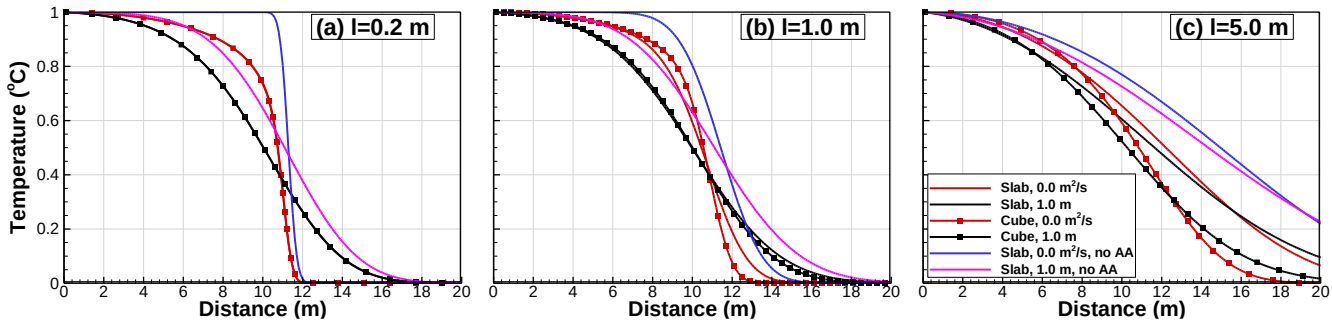

Temperature profiles with radial distance from an injection well, as functions of thermal dispersivity (α_L in m, or effective dispersion coefficient of 0) and shape (slab and cube) and size (fracture spacing of 0.2, 1 and 5 m) of matrix blocks, with a 30 m thick overlying aquitard and a 50 m thick underlying aquitard.

Source: LBNL

Support of Flexible-Mode Operation at The Geysers

The modeling tools were applied in support of flexible-mode production at The Geysers geothermal field. This involved site-specific material properties and conditions, including detailed well design and reservoir conditions for this vapor-dominated site at the southeast Geysers. An important part of this evaluation was to use pilot test data for the flexible-mode production collected by Calpine Corporation during its CEC project on flexible production (EPC-14-002). This pilot test was used for validation of the model through detailed modeling of a production curtailment test. The validated model was then used for modeling and assessment of the long-term impacts of flexible production in the same well.

Model Validation Against Geysers Pilot Test on Production Curtailment

Model validation was conducted against pilot test data on production curtailment obtained from Calpine Corporation. A fully coupled axial symmetric wellbore-reservoir model was developed and a curtailment production test conducted at well 15A28 on May 19, 2015 was simulated for model validation. Details of the well configurations, including casing wall and cement, were explicitly represented in the numerical grid. Four steam entry zones found during drilling were also represented as higher permeability zones in the model.

For estimating temperature and pressure in the well assembly and surrounding rock, production over the 28-year lifetime of the well was simulated by considering monthly production rates. This modeling involved calibration of reservoir permeability and some of the thermal properties of the well assembly to match the observed pressure-flow response and wellhead temperature during the 28 years of production.

The pilot curtailment test at The Geysers well 15A28 on May 19, 2015, was then simulated for model validation. To be consistent with the field operation, production was reduced by simulating closure and reopening of a valve. By reducing the cross-sectional area to 20 percent, the mass flow rate was reduced by about 40 percent, from 40 to 25 kph (Figure 3-30a). The model captured major features in the steam production rate (Figure 3-30a), temperature, and pressure (Figure 3-30b), although the simulated responses were a bit more abrupt than what was observed in the field. The pressure within the well changed by about 0.5 MPa, while a few degrees temperature change occurred at the wellhead. These changes in pressure and temperature were quite small but useful for validating the model regarding pressure and temperature responses during typical curtailment of a production well.

Further model validation was provided by comparing predicted and measured temperature and pressure profiles along the well during the curtailment experiment (Figure 3-31). Depth-dependent pressure and temperature data were obtained by moving sensors downward during 09:17:21 – 10:07:20 (conventional production rate) and upward during 14:45:10 – 16:06:14 (reduced production rate). The solid blue line is the profile output at 11:39:54 to indicate the changing profile during reduced production (11:30:24 – 16:31:24). Nevertheless, the overall agreement in simulated and measured data provided confidence in the modeling of temperature and pressure responses, and the model was validated for further sensitivity studies related to flexible production.

Figure 3-30: Simulated and Measured Pilot Test Response

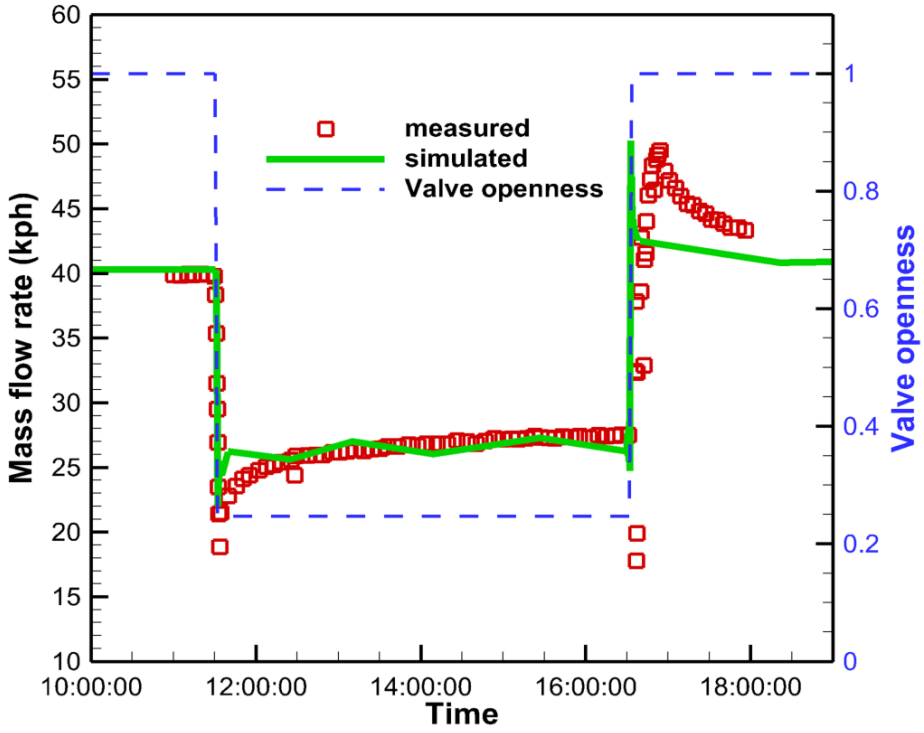

(a)

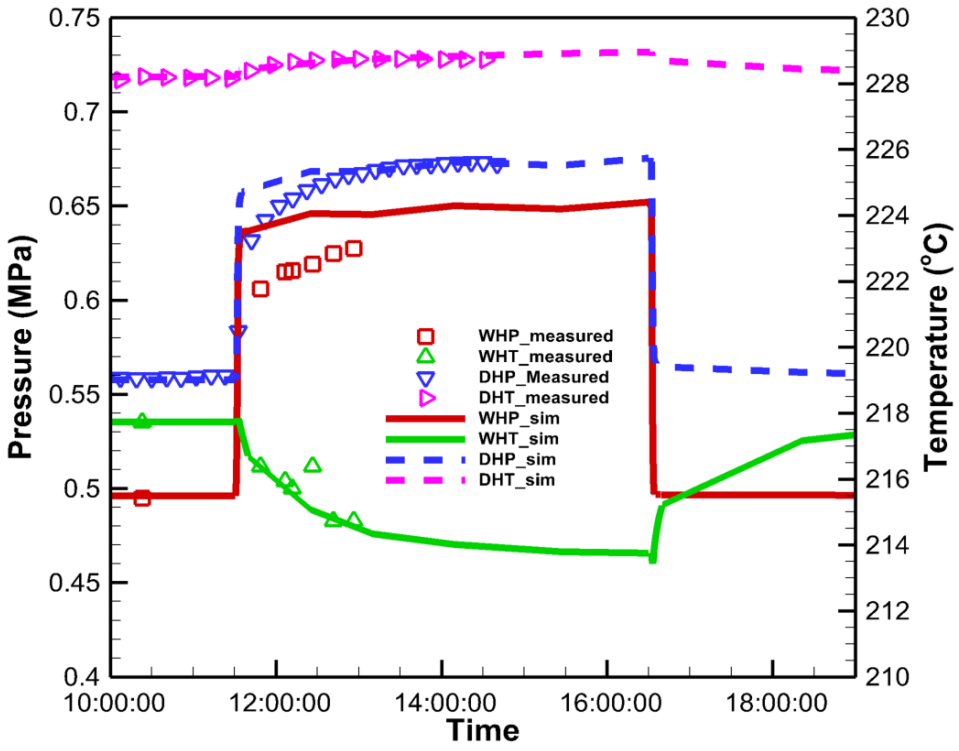

(b)

Simulated and measured (a) mass flow rate and (b) pressure and temperature. Symbols are measured data while lines are model simulation results.

Source: LBNL

Figure 3-31: Simulated and Measured Pilot Test Results With Depth

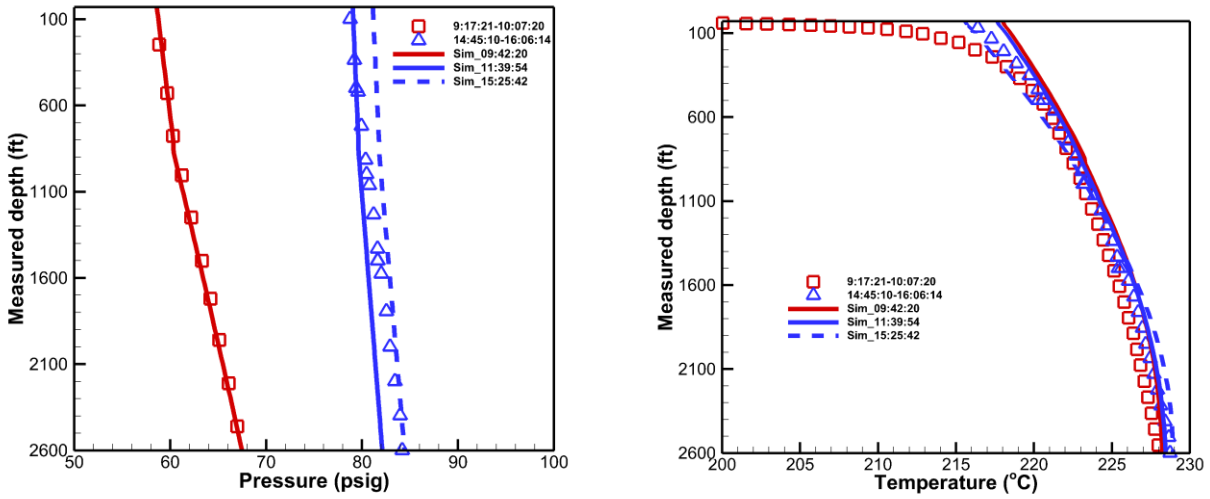

Simulated and measured vertical profiles of (a) pressure and (b) temperature

Source: LBNL

Overall, modeling of the pilot curtailment test well 15A28 showed that the calibrated model is capable of reproducing observed wellhead pressure and temperature, downhole (2,600') pressure and temperature, and the production rate during curtailment. The major fitting parameters were the reservoir permeability, ambient reservoir pressure and temperature, the openness of the valve that controls the production rate at surface, and the heat conductivity of cement and cap rocks. Curtailment-induced changes in pressure and temperature were relatively small. Finally, the simulations showed that no liquid phase occurred in the well during the curtailment experiment in this well in the steam-dominated reservoir. This is important since condensed water could cause corrosion of the well casing.

Assessment of Flexible-Mode Production at Southeast Geysers

Based on the site-specific model developed and validated against the pilot test, the research team conducted simulations to predict long-term changes and risks of flexible-mode production, which complemented observations from the short-time pilot tests. This modeling evaluated coupled reservoir-wellbore modeling for long-term wellbore integrity, geochemical modeling for corrosion of the production wells, and thermal and hydraulic modeling of the wellbore and reservoir for impacts from both injection and energy production. The simulations were conducted for 100 days of daily cyclic production including 12 hours of daily production at a peak rate of 40 kph. Two cases of daily cycles were considered: in the first case with half-cut cycles (reducing production to 50 percent) during 12 hours and in the other case with complete shut-in during 12 hours.

Mechanical Changes in the Well Assembly

The calculated pressure and temperature evolution within the cement behind the 11" casing is shown in Figures 3-32 and 3-33. In both cases, the responses reach quasi regular patterns after about one month of cyclic production. The magnitudes of pressure and temperature

variations in the case with shut-in cycles were much larger than the case with only half-cut cycles. For example, in the case of shut-in cycles, the temperature in the cement at 266 m fluctuated more than 20°C, whereas in the case of half-cut cycles, the temperature only varied by about 2°C. The change in cement pressure induced by cyclic production at shallow depths (266 and 499 m) was not significant. In the cement near the bottom of the 11" casing (786 m), the pressure changed with the production rate because it was near the reservoir, which was under cycling pressure change. The magnitude of pressure changes in the shut-in case was much larger than in the half-cut case but with only 0.1 MPa variations, which are small.

Figure 3-32: Simulated Cement Temperature During Cyclic Production

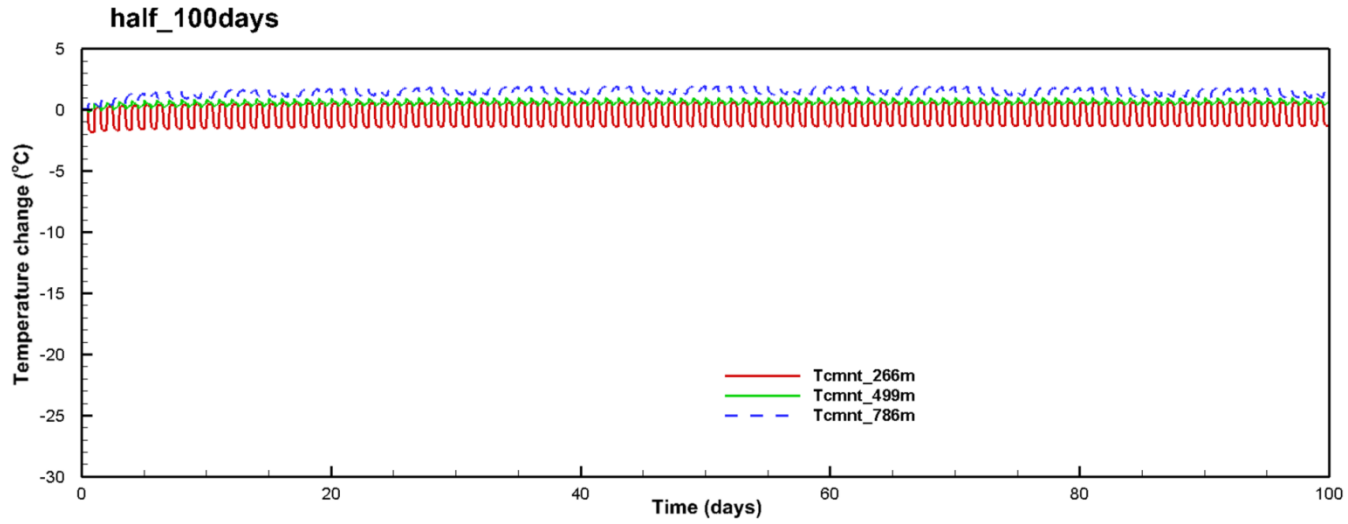

(a)

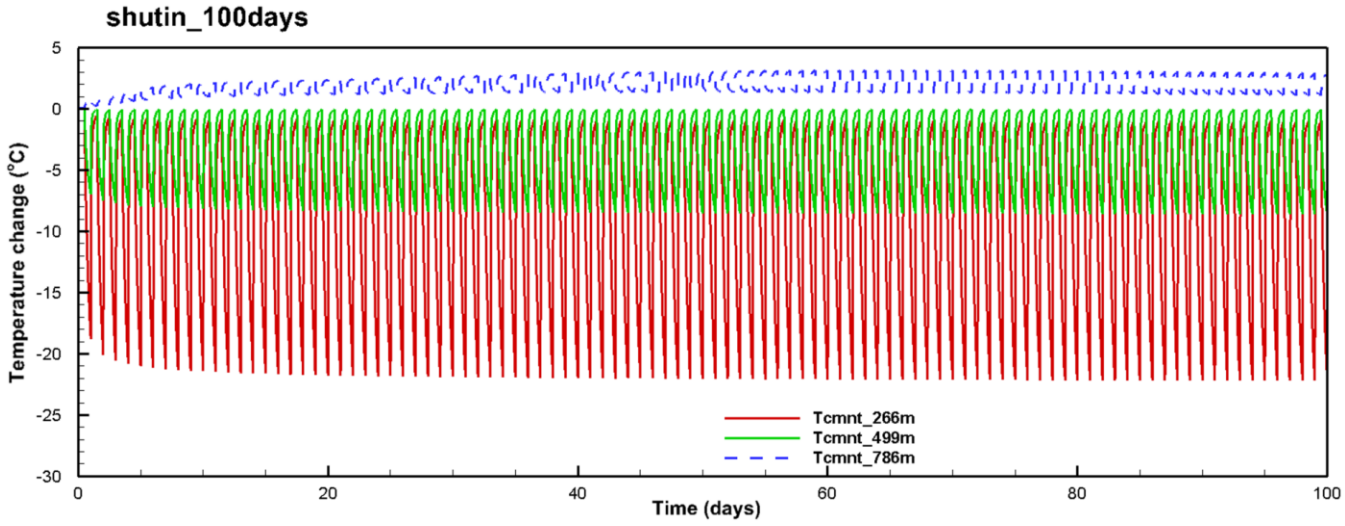

(b)

Well temperature evolution at different depths during 100 days of cyclic production in the case of (a) half-cut production cycles and (b) shut in production cycles.

Source: LBNL

Figure 3-33: Simulated Cement Pressure During Cyclic Production

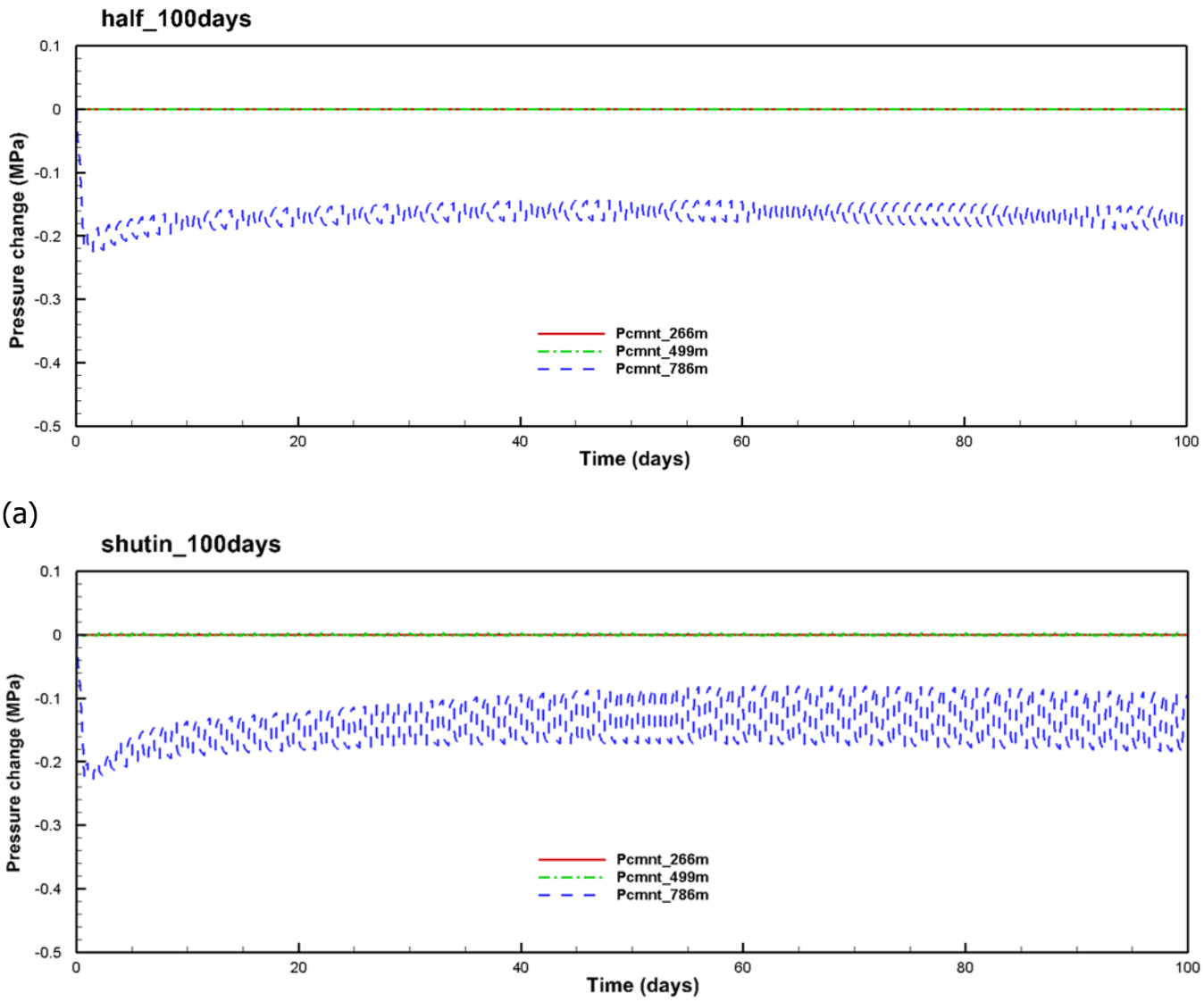

Pressure evolution in the cement at different depths during 100 days of cyclic production in the case of (a) half-cut production cycles and (b) shut in production cycles.

Source: LBNL

Figure 3-34 shows the calculated stress evolution during cyclic production in the cement just behind the casing. The results are for locations close to the ground surface (10 m depth) and at the top of the 11-inch casing, at 266 m depth. In the case of half-cut cyclic production, the stress cycles were very small compared with initial stress increases during system startup (Figure 3-34a). In the case of cyclic production with shut-in cycles, the stress cycles were much more significant, with stress cycles of about 5 MPa (Figure 3-34b). The big difference in the mechanical impact on the wells for half-cut and shut-in production cycles shows the importance of keeping hot fluid flowing to some degree and to avoid cooling the wells, which could occur if production were completely shut down during low-production cycles.

Figure 3-34: Simulated Stress During Cyclic Production

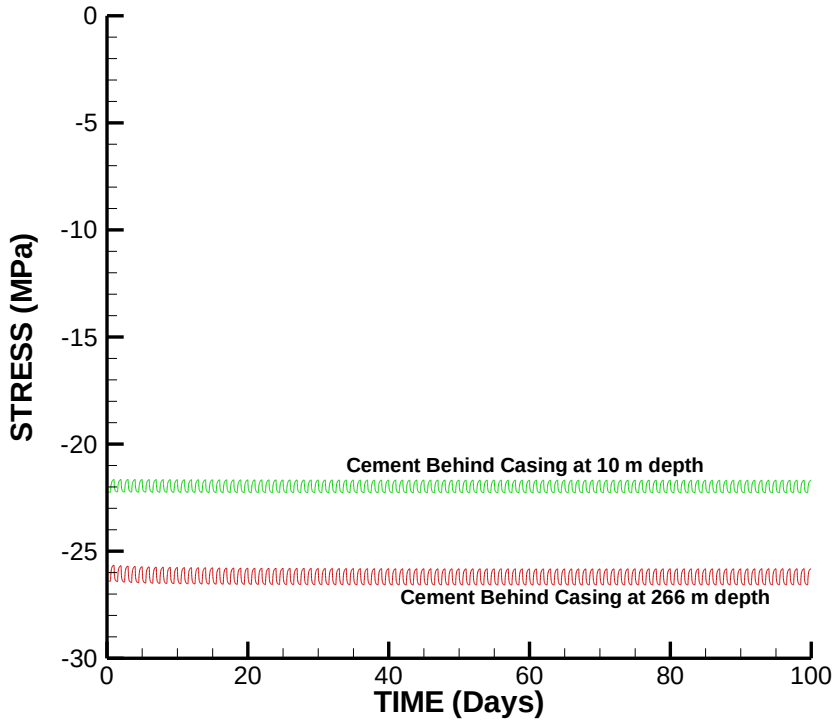

a))

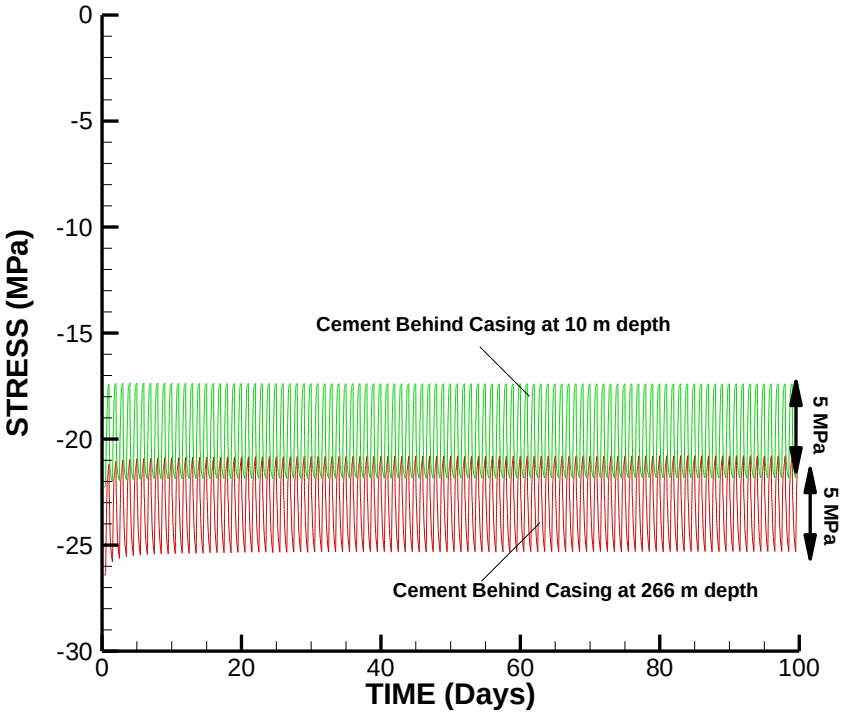

Calculated stress evolution in cement behind casing for (a) half-cut cyclic production and (b) shut-in cyclic production.

Source: LBNL

Impact on Scaling and Corrosion

Mineral scaling is typically not an issue for vapor-dominated systems such as The Geysers. However, corrosion by HCl is of concern in some areas of The Geysers where HCl is present in superheated steam, even at low concentrations (10-150 ppm) (Haizlip and Truesdell, 1988; Truesdell et al., 1989). Because HCl partitions very strongly in the aqueous phase, minute amounts of steam condensate can scrub enough HCl from the vapor phase to yield strongly acidic condensate, which then can drive well corrosion if the condensation takes place on the casings (Haizlip and Truesdell, 1991). The effect of flexible production mode on condensation therefore needs to be carefully examined since it directly relates to potential HCl corrosion.

Cyclic increases in pressure could possibly increase corrosion potential if condensation occurs in the well. Conversely, increased condensation by vapor adsorption on mineral surfaces and capillary condensation in small pores in rocks surrounding production wells could scavenge and neutralize HCl away from the wells, lowering the corrosion potential (Pruess et al., 2007). Under the flexible production mode considered in this study, vapor was not predicted to condensate within wells unless the wells were fully shut-in. In this case condensate was predicted to form at ~20 m below the wellhead, with a very small volumetric saturation (< 0.001). For this reason, cyclic production is not expected to increase the potential for HCl corrosion in wells, except in cases of complete shut-in, which is not a recommended scenario. The potentially beneficial effect of increased condensation by cyclic pressure increases (thus increased HCl scrubbing) at locations away from wells merits further investigation.

CHAPTER 4: Technology/Knowledge/Market Transfer Activities

The project team at LBNL developed materials that advanced technology transfer including project fact sheets, reports, conference and journal articles, and presentation materials. The modeling tools developed in this project, namely the routines for performing well integrity and reservoir analyses, have been documented in reports and scientific articles and presented at conferences. The users of these modeling tools are scientists and engineers familiar with analytical and numerical modeling of subsurface thermal, hydraulic, and geomechanical processes. To communicate the methods, technologies, and learnings developed in this project, a number of technology/knowledge transfer activities were planned and implemented, as described here.

Website

The project was introduced at LBNL Earth and Environmental Sciences Area (EESA) web site:

https://eesa.lbl.gov/projects/comprehensive-physical-chemical-modeling-to-reduce-risks-and-costs-of-flexible-geothermal-energy-production-epic/

Written Documents

Written documents include technical reports and published papers, summarized here.

Reports to CEC

The main project reports submitted to the CEC were annual reports, including *Development of Coupled Reservoir-Wellbore THMC Modeling Tools* (Rutqvist et al., 2018a), *Impacts and Technical Risks Associated with Base-Load and Flexible Production in Liquid-Dominated Geothermal Reservoirs* (Rutqvist et al., 2019), and *Application of the Coupled Reservoir-Wellbore THMC Modeling to Support Flexible-Mode Operation of the Geysers Geothermal Field* (Rutqvist et al., 2020b). The final report provides a summary of the results in these annual reports.

Modeling Tools Report and User's Manuals

The following modeling tools report and users' manuals describe the modeling tools and how to use them, including *Development of Coupled Reservoir-Wellbore THMC Modeling Tools* (Rutqvist et al., 2018a), *User's Manual for Coupled T2WELL-FLAC3D Simulations* (Rutqvist et al., 2018d), *User's Manual for Multi-rate Heat Transfer Simulators* (Zhou and Rutqvist, 2018). These are provided to potential users upon request.

Conference and Journal Papers

A number of conference and journal papers present the modeling tools, results, and findings from the modeling studies related to flexible mode geothermal production. The T2WELL-FLAC3D model was presented in a conference paper to the 2018 TOUGH Symposium (Rutqvist et al., 2018b), while results related to well integrity were presented in conference papers to

the 2018 and 2020 Stanford Geothermal Workshops (Rutqvist et al., 2018a; 2020a), as well as in a conference paper for the 2021 World Geothermal Congress (Rutqvist et al., 2021). The SHPALib modeling tool and its application to modeling heat transport with fracture-matrix interactions were presented in a conference paper at the 2018 Stanford Geothermal Workshop (Zhou et al., 2018), as well as in three journal papers (Zhou et al., 2017a, b; 2019).

Presentations and Discussions

The LBNL team presented findings at:

(1) The 2018 Stanford Geothermal Workshop, Stanford University, Stanford, California.

(2) The 2018 TOUGH Symposium, Lawrence Berkeley National Laboratory, Berkeley, California.

(3) The 2020 Stanford Geothermal Workshop, Stanford University, Stanford, California.

(4) The 2020+1 World Geothermal Congress, Reykjavik, Iceland (virtual).

The Stanford Geothermal Workshop and the World Geothermal Congress were attended by representatives from industry, academia, and government agencies. The presentations were well attended and of interest to many operators (as revealed by the discussions following the presentations). The 2020 Stanford Geothermal Workshop took place in person in February 2020, just before the pandemic prevented in-person workshops and presentations. The 2020+1 World Geothermal Congress was held virtually in May 2021. Participants at the 2018 TOUGH Symposium were scientists and engineers who are the users of the TOUGH family of multiphase flow simulators, including T2WELL. They are likely users of the modeling tools developed in this project.

Discussions and meetings have been carried out with Calpine Corporation, as well as with Ormat. Representatives of these and other organizations also attended the 2018 and 2020 Stanford Geothermal Workshops and the 2020+1 World Geothermal Congress. Moreover, representatives from both Calpine and Ormat were part of the Technical Advisory Committee for this project.

CHAPTER 5:
Conclusions/Recommendations

Conclusions

Numerical modeling tools were developed and implemented to study the impacts of flexible-mode geothermal energy production on technical challenges including well integrity, reservoir performance, and scaling and corrosion in production wells. Modeling simulations for both baseload and flexible geothermal energy production were performed for both steam- and liquid-dominated geothermal systems in California.

- Temperature fluctuations could lead to negative impacts on well integrity and reservoir performance, as well as mineral scaling and casing corrosion.
- The highest thermal perturbation and stress changes occurred in production wells at shallow depth, just below the ground surface.
- Temperature changes in the cement behind the casing can cause significant and potentially damaging fluid pressure changes from thermal expansion of trapped fluids.
- Changes in temperature and fluid pressure cause stress and strain changes that could cause mechanical failure in casing, cement, and adjacent rock.
- It was found that the biggest risk of mechanical failure occurs during the initial start-up of production because of large and rapid temperature increases from initially cool temperatures near the ground surface.
- During variable production with daily production cycles, temperature fluctuations also caused fluctuations in pore pressure and stress, with relatively larger impact when producing from a very hot steam-dominated system.
- If production cycling is carefully controlled (e.g., ramping up production slowly and not completely shutting down production), then impacts to the well assembly can be minimized.
- For a liquid-dominated system, mineral scaling and corrosion can be controlled by maintaining wellhead pressure above the saturation pressure while at the same time keeping the temperature above the silica saturation temperature.
- In a steam-dominated system, scaling is typically not a concern, and corrosion can be avoided by avoiding condensation that could occur during prolonged production curtailments.

Recommendations:

The modeling tools developed and demonstrated in this project can be applied to any new geothermal sites to develop site-specific operational strategies for safe, variable geothermal production at reduced costs. These strategies will depend on site-specific conditions such as whether the system is steam or liquid dominated, fluid chemistry, well design, depth, and reservoir temperature. As demonstrated in this research, the modeling tools can be used to determine how fast and how much production can be increased or decreased to prevent rapid temperature changes and potentially damaging thermal pressurization of trapped fluids.

Longer-term shut-in of production should be avoided if possible as this can give rise to 2-phase fluid flow conditions and potential corrosion in the well, and could lead to large temperature increases and stress during subsequent startups. Moreover, long-term shut-ins can reduce temperatures below the silica saturation temperature and therefore cause mineral deposition. Using this approach, guidelines can be developed for safe and cost-effective steady or variable-rate production from geothermal production wells.

CHAPTER 6:
Benefits to Ratepayers

This project provides geothermal energy producers with tools and guidelines that can lead to greater grid reliability, increased use of intermittent renewable energy, reductions in GHG emissions, lower costs, and other benefits to California ratepayers.

Reliability

Geothermal power plants, which generated 6 percent of California's in-state electricity in 2020, can operate in several variable modes including for grid support, regulation, load following, spinning reserve, non-spinning reserve, and replacement reserve. Increasing flexible-mode operation of geothermal power plants may reduce peak power generation from existing natural gas-fired power plants. Moreover, flexible-mode geothermal energy production would allow for better use of the current installed capacity of 2,712 megawatts from a total of 40 operating geothermal power plants in California. Indeed, California geothermal plants generated 11,345 gigawatt-hours (GWh) of electricity in 2020, indicating that about 48 percent of the capacity is in operation year-round (note that the capacity factor for these plants vary significantly from field to field (Robertson-Tait et al., 2021). The fairly low reported cumulative capacity factor for the state's geothermal fields is mostly due to long-term declines in steam production in the case of The Geysers, and brine production in the case of Coso (Sanyal and Enedy, 2016; Eneva et al., 2018); most other fields in California have capacity factors greater than 80 percent. Electrical generation data for California reported in this section are from the California Energy Commission's Energy Almanac for 2020 entitled "Total System Electric Generation" (CEC, 2021).

Lower Costs

The lower cost of flexible-mode geothermal energy production can be understood by comparing the following two cases. In the first case, geothermal energy is continuously generated in baseload mode, and subsurface energy storage technologies store excess renewable energy that can be used when needed on a daily basis. Such technologies include compressed air energy storage (CAES) and aquifer thermal energy storage (ATES). The additional cost for such energy storage will be significant, including site selection and characterization, operation and monitoring, and environmental impacts. In the second case, existing geothermal energy power plants are switched to flexible-mode operation; their energy is supplied only when needed. At all other times, the geothermal energy can be preserved underground in the well-characterized and well-operated fields with no additional cost for preservation. In addition, the installed capacity can be used during the supply hours. The importance and the cost effectiveness of flexible-mode geothermal production will become progressively attractive as intermittent renewable energy increasingly dominates California's energy supply. The main disincentive is that most geothermal fields are designed to operate at a near-constant high rate of production, and variable production usually means curtailment of production (and loss of revenue) when less energy is required by the grid (Dobson et al., 2020). These losses could be compensated by contractual incentives for flexible generation to

balance the needs of the grid, or by avoidance of the financial impacts of negative pricing when there is an overabundance of energy production (Millstein et al., 2021).

Quantitative Benefits

The quantitative benefits of this project, including ratepayer benefits of lowered operating costs, depend on two key factors. The first factor is how the flexible-mode production will operate daily and seasonally including the curtailed production rate and duration and the peak production rate and duration. Due to the limits of reservoir pressure and maximum capacity of production rate, the peak rate for flexible-mode production can be slightly higher than for the constant production rate in baseload mode. This means the total annual electricity generation for the former could be smaller than for the latter. The second factor is how geothermal power plants that adopt flexible-mode production will be paid. The day-ahead, 15-minute, and 5-minute prices for net load varies yearly and month by month (California ISO, 2021, Figure E.1). The hourly load-weighted average energy prices (January through March, 2021) in California also vary significantly (see Figure 6-1), with minimum and maximum prices of $16 and $87/MWh, respectively. When switching from constant baseload production to a flexible-mode production with eight hours of full shut-in, geothermal power plants will lose 18 percent of their revenue. With the 30 percent off-peak production rate used in this project's modeling, the revenue loss is 13 percent. This means that flexible-mode production (with a 30 percent off-peak production rate for eight hours and a 107 percent peak production rate relative to the constant baseload production rate), will not suffer revenue loss. This slight production rate increase from the constant rate is very reasonable (Goyal, 2002). For this hypothetical 30- to 107-percent combination of flexible-mode production, only 81 percent production would be required compared with baseload mode, so the geothermal reservoir would undergo slower depletion and last longer for future generation. Note that for most geothermal power plants, pricing is set by power purchase agreements rather than by the spot market, so such agreements would need to provide incentives for flexible generation as an ancillary value to both the grid and the offtaker (Thomsen, 2018; 2021).

The many benefits of flexible-mode production to the increasing use of intermittent renewables in California need to be considered in long-term (rather than daily or minute) contracts to incentivize flexible geothermal power plants. With these incentives and rewards for higher contractual prices, the conversion to flexible-mode geothermal power generation will be financially beneficial. The team followed the economic assessment conducted by Edmunds et al. (2014) and Edmunds and Sotorrio (2015). For example, consider a contract to provide energy at a firm contract price of $50/MWh (rather than the average price of $44 shown in Figure 6-1). Assuming a 100-percent capacity factor for 1 MW of capacity (with 30 percent off-peak and a 107-percent peak rate), annual revenues from energy-only sales would be 8,760 hours x $50/MWh x 1.0 =$438,000 per year. At this long-term contract price, the team's calculations show an increase of $52,560 in annual revenue, with 12 percent higher revenue than in baseload mode. Considering that the geothermal capacity in operation is 1,295 MW with 11,345 gigawatt-hours (GWh) of electricity produced in 2020, the total net revenue by switching to ancillary services under a contractual system that rewards off-peak generation would be $68.1M. Intermittent renewable resources will also increase significantly over the next decades and become more cost-effective with time. Flexible-mode geothermal energy would make their increased use possible and feasible without additional cost of

subsurface energy storage or other-type energy storage. These are qualitative benefits. A more detailed evaluation of potential flexible production scenarios is presented in Millstein et al. (2021).

The commercial and technical viability of flexible geothermal operations have been demonstrated at the Puna Geothermal Venture plant in Hawaii since 2012. This plant, the first of its kind, provides ancillary services for grid support that are identical to those of existing oil-fired peak generating resources on Hawaii's Big Island (Nordquist et al., 2013).

Figure 6-1: Hourly Load-Weighted Average Energy Price

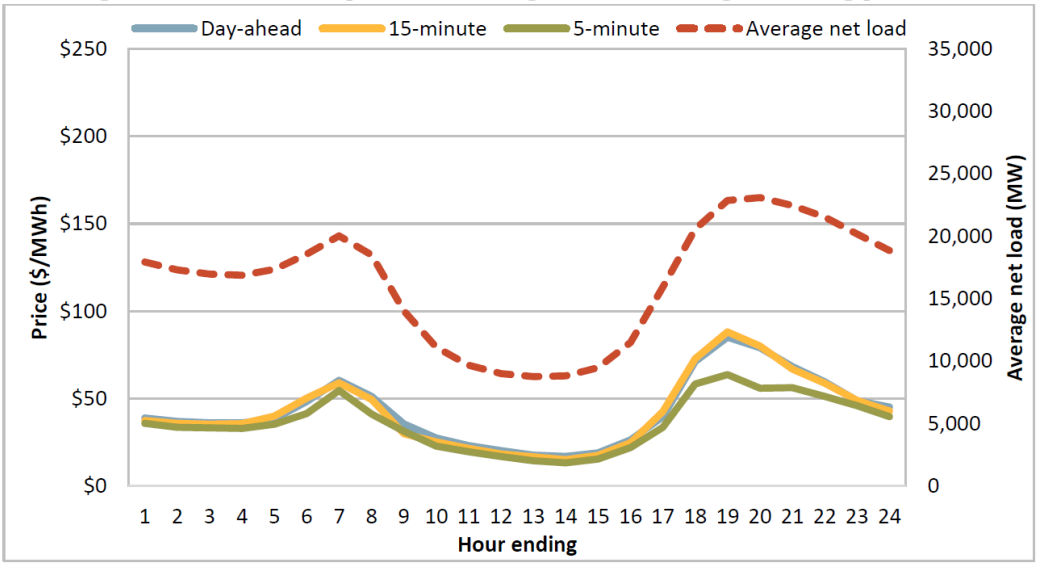

Hourly Load-Weighted Average Energy Price (January – March, 2021) (California ISO, 2021).

Source: LBNL

Cost Benefits

This project could provide a rapid return on investment for California customers and project stakeholders including the California Public Utilities Commission and the state's investor-owned utilities. If this project's recommendations were adopted by just 10 percent of the geothermal energy sector (together with power sales contracts that incentivize flexible-mode generation), annual energy cost savings in California would total $6.8M in this hypothetical scenario, and the payback period would be around two months. Although compelling, this cost-benefit would not likely prompt the private sector to develop the tools required to achieve these results, since it will require specialized mathematical model development that is not readily available to geothermal operators. In addition, the expected benefits of sustainable geothermal energy generation, which is a natural feature of flexible-mode operation, are more significant than the energy cost savings. Flexible-mode geothermal energy production could lead to longer productive lives of geothermal fields.

GLOSSARY AND LIST OF ACRONYMS

Term	Definition
ΔT	Temperature perturbation, delta-T, or change in temperature
ATES	Aquifer thermal energy storage
CEC	California Energy Commission
CAES	Compressed air energy storage
GPM	Gallons per minute
GHG	Greenhouse gas
FLAC3D	Fast Lagrangian Analysis of Continua in 3 Dimensions
kg	Kilograms
kg/s	Kilograms per second
LBNL	Lawrence Berkeley National Laboratory
m	Meters
MPa	Megapascals
NCG	Non-condensable gases
Scaling	Mineral precipitation and build-up of mineralization inside a well
T2WELL	A numerical simulator for non-isothermal, multiphase, and multi-component flows in the integrated wellbore–reservoir system based on TOUGH2
TAC	Technical advisory committee
TDS	Total dissolved solids
TH	Thermal-hydrological
THM	Thermal-hydrological-mechanical
THMC	Thermal-hydrological-mechanical-chemical
TOUGH	Transport of unsaturated groundwater and heat – a suite of software codes
TOUGH2	A general-purpose numerical simulation program for multi-dimensional fluid and heat flows of multiphase, multicomponent fluid mixtures in porous and fractured media

Term	Definition
TOUGHTRECT	A simulation program for non-isothermal multiphase reactive geochemical transport in variably saturated geologic media based on TOUGH2

REFERENCES

Arnorsson, S., 1989. Deposition of calcium carbonate minerals from geothermal waters, theoretical considerations. Geothermics 18(1/2), 33–39.

California ISO (California Independent System Operator), Q1 2021 Report on Market Issues and Performance, Prepared by: Department of Market Monitoring

CEC (California Energy Commission), 2021, Energy Almanac, 2020 Total System Electric Generation, https://www.energy.ca.gov/data-reports/energy-almanac/california-electricity-data/2020-total-system-electric-generation

Criaud, A., and C. Fouillac, 1989. Sulfide scaling in low enthalpy geothermal environments: a survey. Geothermics 18(1/2), 73–81.

Dobson, P., D. Dwivedi, D. Millstein, N. Krishnaswamy, J. Garcia, and M. Kiran, 2020. Analysis of curtailment at The Geysers geothermal Field, California. Geothermics 87, https://doi.org/10.1016/j.geothermics.2020.101871

Edmunds, T.A., P. Sotorrio, and T.A. Buscheck, 2014. Flexible Geothermal Power: An Economic Assessment. FY14 Final Report, LLNL-TR-664520, Lawrence Livermore National Laboratory, Livermore, CA.

Edmunds, T.A., and P. Sotorrio, 2015. Ancillary Service Revenue Potential for Geothermal Generators in California. FY15 Final Report, LLNL-TR-669828, Lawrence Livermore National Laboratory, Livermore, CA.

Eneva, M., A. Barbour, D. Adams, V. Hsiao, K. Blake, G. Falorni, and R. Locatelli, 2018. Satellite observations of surface deformation at the Coso geothermal field, California. Geothermal Resources Council Transactions 42, 19 p.

Farrar, C., J. DeAngelo, L., Clor, F. Murphy, C. Williams, F. Grubb, and S. Hurwitz, 2010. Temperature data from wells in Long Valley Caldera, California. USGS Digital Data Series 523, Version 3.0 (Nov. 2016), https://pubs.usgs.gov/ds/523/. (Temperature data for MBP-3)

Gallup, D., 1989. Iron silicate scale formation and inhibition at the Salton Sea geothermal field. Geothermics 18(1/2), 97–103.

Gallup, D., 2009. Production engineering in geothermal technology: A review. Geothermics 38, 326–334.

Garcia, J., C. Hartline, M. Walters, M. Wright, J. Rutqvist, P.F. Dobson, and P. Jeanne, 2016. The Northwest Geysers EGS Demonstration Project, California - Part 1: Characterization and reservoir response to injection. Geothermics 63, 97–119. https://doi.org/10.1016/j.geothermics.2015.08.003.

Goyal, K.P., 2002. Reservoir response to curtailments at The Geysers. Proceedings, 27th Workshop on Geothermal Reservoir Engineering, Stanford University, Stanford, California, January 28-30, 2002, SGP-TR-171, 7 p.

Haizlip, J.R., and A.H. Truesdell, 1988. Hydrogen chloride in superheated steam and chloride in deep brine at the Geysers geothermal field, California. Proceedings, Thirteenth Workshop on Geothermal Reservoir Engineering, Stanford University, Stanford, California, January 19-21, 1988 - SGP-TR-113.

Haizlip, J.R., and A.H. Truesdell, 1991. Non-condensable gas and chloride are correlated in steam at The Geysers. Geothermal Resources Council, Monograph on The Geysers Geothermal Field, Special Report No. 17, 139–143.

Itasca, 2011. FLAC3D V5.0, Fast Lagrangian Analysis of Continua in 3 Dimensions, User's Guide. Itasca Consulting Group, Minneapolis, Minnesota.

Kaldal, G.S., M.P. Jonsson, H. Palsson, and S. Karlsdottir. 2015. Analysis of Casings in High Temperature Geothermal Wells in Iceland. Proceedings World Geothermal Congress 2015, Melbourne, Australia, 19-25 April 2015.

Kaya, T., and P. Hoshan, 2005. Corrosion and Material Selection for Geothermal Systems. Proceedings World Geothermal Congress 2005, Antalya, Turkey, 24-29 April 2005.

Matek, B., 2015. Geothermal Energy Association Issue Brief: Firm and Flexible Power Services Available from Geothermal Facilities. Geothermal Energy Association, Washington, D.C.

Miller, R.J., and R. Vasquez, 1988. Analysis of production and reservoir performance, Casa Diablo geothermal project. SPE California Regional Meeting, Long Beach, CA, SPE 17426. (Early well production data for MBP-3 and MBP-4)

Millstein, D., P. Dobson, and S. Jeong, 2021. The potential to improve the value of U.S. geothermal electricity generation through flexible operations. J. Energy Resources Tech. 143(1): 010905. doi:10.1115/1.4048981

Ngothai, Y.T., N. Yanagisawa, A. Pring, P. Rose, B. O'Neill, and J. Brugger, 2010. Mineral scaling in geothermal fields: A review. Australian Geothermal Conference 2010, Adelaide.

Nordquist, J., T. Buchanan, and M. Kaleikini, 2013. Automatic generation control and ancillary services. Geothermal Resources Council Transactions 37, 761–766.

Pan, L., and C.M. Oldenburg, 2014. T2WELL—An integrated wellbore–reservoir simulator. Computers & Geosciences 65, 46–55.

Pruess, K., C. Oldenburg, and G. Moridis, 1999. TOUGH2 user's guide. Report LBNL-43134. Lawrence Berkeley National Laboratory, Berkeley, CA, USA.

Pruess, K., N. Spycher, and T.J. Kneafsey, 2007. Water injection as a means for reducing non-condensable and corrosive gases in steam produced from vapor-dominated reservoirs. Proceedings, Thirty-Second Workshop on Geothermal Reservoir Engineering, Stanford University, Stanford, California, January 22-24, 2007 SGP-TR-183.

Reyes, A.G., W.J., Trompetter, K. Britten, and J. Searle, 2002. Mineral deposits in the Rotokawa geothermal pipelines, New Zealand. Journal of Volcanology and Geothermal Research 119, 215–239.

Robertson-Tait, A., W. Harvey, S. Hamm, and L. Boyd, 2021. The United States of America country update 2020 – Power generation. Proceedings World Geothermal Congress 2020+1, Reykjavik, Iceland.

Rutqvist, J., 2011. Status of the TOUGH-FLAC simulator and recent applications related to coupled fluid flow and crustal deformations. Computers & Geosciences 37, 739–750.

Rutqvist, J., 2017. An overview of TOUGH-based geomechanics models. Computers & Geosciences, 108, 56–63. https://doi.org/10.1016/j.cageo.2016.09.007.

Rutqvist J., P. Jeanne, P.F. Dobson, J. Garcia, C. Hartline, L. Hutchings, A. Singh, D.W. Vasco, and M. Walters, 2016. The Northwest Geysers EGS Demonstration Project, California - Part 2: Modeling and interpretation. Geothermics 63, 120–138. https://doi.org/10.1016/j.geothermics.2015.08.002.

Rutqvist J., L. Pan, and M. Hu, 2018b. T2WELL-FLAC3D for advanced well integrity analysis. Proceedings TOUGH Symposium 2018, Berkeley, California, October 8-10, 2018.

Rutqvist, J., L. Pan, and M. Hu, 2018d. User's Manual for Coupled T2WELL-FLAC3D Simulations. Submitted to California Energy Commission (CEC) under agreement EPC-16-022, February 2018.

Rutqvist, J., L. Pan, M. Hu, Q. Zhou, and P. Dobson, 2018c. Modeling of coupled flow, heat and mechanical well integrity during variable geothermal production. Proceedings, 43rd Workshop on Geothermal Reservoir Engineering, Stanford University, Stanford, California, February 12-14, 2018. https://pangea.stanford.edu/ERE/pdf/IGAstandard/SGW/2018/Rutqvist.pdf.

Rutqvist J., L. Pan, N. Spycher, P. Dobson, Q. Zhou, and M. Hu, 2020a. Coupled Processes Analysis of Flexible Geothermal Production from Steam- and Liquid-Dominated Systems: Impact on Wells. Proceedings, 45th Workshop on Geothermal Reservoir Engineering Stanford University, Stanford, California, February 10-12, 2020.

Rutqvist, J., L. Pan, N. Spycher, P. Dobson, Q. Zhou, and M. Hu, 2021. Coupled Processes Analysis of Flexible Geothermal Production from a Liquid-Dominated Geothermal System: Impact on Wells. Proceedings World Geothermal Congress 2020+1, Reykjavik, Iceland.

Rutqvist, J., L. Pan, N. Spycher, Q. Zhou, P. Dobson, and M. Hu, 2020b. Application of the Coupled Reservoir-Wellbore THMC Modeling to Support Flexible-Mode Operation of the Geysers Geothermal Field. Report to California Energy Commission (CEC) under agreement EPC-16-022. Feb 12, 2020.

Rutqvist, J., Q. Zhou, L. Pan, M. Hu, N. Spycher, and P. Dobson, 2018a. Development of Coupled Reservoir-Wellbore THMC Modeling Tools: Report to California Energy Commission (CEC) under agreement EPC-16-022. February 12, 2018.

Rutqvist, J, Q. Zhou, L. Pan, N. Spycher, and P. Dobson, 2019. Impacts and Technical Risks Associated with Base-Load and Flexible Production in Liquid-Dominated Geothermal Reservoirs. Report to California Energy Commission (CEC) under agreement EPC-16-022. May 13, 2019.

Sanyal, S.K., and S.L. Enedy, 2016. Fifty-five years of commercial power generation at The Geysers geothermal field, California: the lessons learned. In: DiPippo, R. (Ed.), Geothermal Power Generation. Woodhead Publishing, 591–608.

Sonnenthal, E., N. Spycher, T. Xu, L. Zheng, N. Miller, and K. Pruess, 2014. TOUGHREACT V3.0-OMP reference manual: A parallel simulation program for non-isothermal multiphase geochemical reactive transport. Lawrence Berkeley National Laboratory, Berkeley, CA.

Spycher, N.F., and M.H. Reed, 1989. Evolution of a Broadlands-type epithermal ore fluid along alternative P-T paths: implications for the transport and deposition of base, precious, and volatile metals. Economic Geology 84, 328–359.

Spycher N.F., and M.H. Reed, 1992. Microcomputer-based modeling of speciation and water-mineral-gas reactions using programs SOLVEQ and CHILLER. In Water-Rock Interaction (Kharaka and Maest, eds.), Balkema, Rotterdam, 1087–1090.

Teodurio, C., 2015. Why and when does casing fail in geothermal wells: a surprising question? Proceedings World Geothermal Congress 2015, Melbourne, Australia, 19-25 April 2015.

Thomsen, P., 2018. The increasing comparative value of geothermal in California – 2018 edition. Geothermal Resources Council Transactions 42, 2126-2134.

Thomsen, P., 2021. The increasing comparative value of geothermal in California – Trends and forecasts for mid-2019. Proceedings World Geothermal Congress 2020+1, Reykjavik, Iceland, April – October, 2021, 10 p.

Truesdell, A.H., J.R. Haizlip, H. Armannsson, and F. D'Amore, 1989. Origin and transport of chloride in superheated geothermal steam, Geothermics, 18(1/2), 295–304.

Urbank, K., and A. Jorgensen, 2016. Investigating flexible generation at The Geysers. Geothermal Resources Council Bulletin, Sept.-Oct., 36–39.

Xu, T., Y. Ontoy, P. Molling, N. Spycher, M. Parini, and K. Pruess, 2004. Reactive transport modeling of injection well scaling and acidizing at the Tiwi field, Philippines. Geothermics 33, 477–491.

Xu, T., N. Spycher, E. Sonnenthal, G. Zhang, L. Zheng, and K. Pruess, 2011. TOUGHREACT Version 2.0: A simulator for subsurface reactive transport under non-isothermal multiphase flow conditions. Computers & Geosciences 37, 763–774.

Zhou, Q., C.M. Oldenburg, J. Rutqvist, and T.J. Kneafsey, 2018. Analytical and Numerical Modeling of Heat Transport in Fractured Reservoirs. Proceedings, 43rd Workshop on Geothermal Reservoir Engineering, Stanford University, Stanford, California, February 12-14, 2018. https://pangea.stanford.edu/ERE/pdf/IGAstandard/SGW/2018/Zhou2.pdf.

Zhou, Q., C.M. Oldenburg, and J. Rutqvist, 2019. Revisiting the analytical solutions of heat transport in fractured reservoirs using a generalized multirate memory function. Water Resources Research 55, 1405–1428. https://doi.org/10.1029/2018WR024150.

Zhou, Q., C.M. Oldenburg, J. Rutqvist, and J.T. Birkholzer, 2017. Revisiting the fundamental analytical solutions of heat and mass transfer: The kernel of multirate and multidimensional diffusion. Water Resources Research 53, 9960–9979. https://doi.org/10.1002/2017WR021040.

Zhou, Q., C.M. Oldenburg, L.H. Spangler, and J.T. Birkholzer, 2017. Approximate solutions for diffusive fracture-matrix transfer: Application to storage of dissolved CO_2 in fractured rocks. Water Resources Research 53(2), 1746–1762, https://doi.org/10.1002/2016WR019868

Zhou, Q., and J. Rutqvist, 2018. User's Manual for Multi-rate Heat Transfer Simulators. Submitted to California Energy Commission (CEC) under agreement EPC-16-022, February 2018.